RICE UNIVERSITY

Characterization of Friction Reducer Properties in Oil-Field Operations

By

Valerie Bolanos Ellis

A THESIS SUBMITTED
IN PARTIAL FULFILLMENT OF THE
REQUIREMENTS FOR THE DEGREE

Master of Science

APPROVED, THESIS COMMITTEE

Mason Tomson, Chair, Professor
Civil & Environmental Engineering

Pedro Alvarez, Dept. Chair, Professor
Civil & Environmental Engineering

Philip Bedient, Professor
Civil & Environmental Engineering

Ross Tomson, President
Shale Water Research Center

HOUSTON, TEXAS

January 2015

Abstract

Characterization of Friction Reducer Properties in Oil-Field Operations

By

Valerie Bolanos Ellis

Friction reducers are essential additives used to economically achieve the high pumping rates required for slickwater fracturing. Decreased friction reducer performance in high-TDS brines has been a major challenge for reusing produced water in hydraulic fracturing. Little work has been done to identify the specific parameters that affect polymeric friction reduction. This research uses friction flow loop experiments to characterize the performance of partially hydrolyzed polyacrylamide friction reducers in conditions relevant to the oil field. Polymer concentration and degree of hydrolysis effects on friction reduction are evaluated in the ranges of 0.25-2 gpt and 0-30%, respectively. The decrease in friction reducer performance is measured in brines up to 120,000 mg/L TDS with varying multivalent cation concentrations. The friction reducer interactions with Na^{+}, Ca^{2+}, Mg^{2+}, Fe^{3+}, and Al^{3+} ions are individually assessed. The results are compared to experiments with a commercial friction reducer, and used to propose an empirical model to predict friction reducer performance based on water composition.

Acknowledgements

It is with immense gratitude that I acknowledge the support and help of my advisors, Shale Water Research Center, my friends, and family during my research. I wish to thank, first and foremost Dr. Mason Tomson, my co-advisor, whose invaluable insight and expertise were critical for the completion of this thesis. He patiently guided and taught me through tough research questions, and his help formed an integral part of this research project.

Second, I would like to thank Ross Tomson at Shale Water Research Center (SWRC) for all of his help. This project would not have been completed without the resources of Shale Water Research Center, his guidance, and financial support of the friction flow loop. To all of the scientists at SWRC, in particular Paula Guraieb and Syed Razavi, thank you for taking the time to help me with this project.

Third, I would like to thank Dr. Amy Kan, and all of the researchers in Dr. Tomson's lab. Dr. Fangfu Zhang, Zhaoyi Dai, and Dr. Narayan Bandari who gave me a lot of advice and suggestions that formed an important part of my thesis. And many thanks to all other lab members Dr. Fei Yan. Lu Wang, Ya Liu and Zhang Zhang for your constant support and encouragement.

Last but not least I would like to thank my co-advisor Dr. Pedro Alvarez for his constant guidance and support. Thank you to all financial support Brine Chemistry Consortium of Rice University, and Shale Water Research Center.

This study would not have been possible without all the help and support from my advisors, friends, family, and sponsors. Great thanks to all of you.

Table of Contents

Abstract ..... **I**

Acknowledgements ..... **II**

List of Figures ..... **VII**

List of Tables ..... **VIII**

Chapter 1: Introduction **1**

1.1 Problem Statement 1

1.2 Purpose of the study 2

Chapter 2: Background and Literature Review **4**

2.1 Introduction to Friction Reducers 4

2.2 Friction Reduction Mechanism 5

2.2.1 General Conclusions from the Literature *5*

2.2.2 Fluid Mechanics *7*

2.2.3 Characteristics of Friction Reducing Flow *14*

2.3 Polymer Degradation Mechanisms 20

2.3.1 Importance of polymer coil size, ionic groups, and linearity *20*

2.3.2 Shear Degradation Mechanisms *20*

2.3.3 Radical Chain Degradation *21*

2.3.4 Monovalent Cation Electrostatic Effect on Radius of Gyration *22*

2.3.5 Crosslinking and Hydrogen Bonding with Multivalent Cations *24*

2.4 Slickwater Hydraulic Fracturing 25

2.4.1 Introduction to Slickwater Fracturing *25*

2.4.2 Additives and Fracturing Process *26*

2.4.3 Inverse Emulsions and the Process of Inversion *27*

2.4.4 Produced Water Composition *28*

Chapter 3: Materials and Methods **30**

3.1 Materials 30

3.1.1 Fracturing Additives *30*

3.1.2 Water Composition *30*

3.2 Friction Flowloop 32

Chapter 4: Results and Discussion 36

4.1 Results 36

4.1.1 Paper Overview 36

4.1.2 HPAM Degree of Hydrolysis 36

4.1.3 Concentration Effects on Friction Reducer Performance 38

4.1.4 Effects of Water Quality on Friction Reduction 39

4.2 Discussion 44

4.2.1 Discussion on Experimental Results 44

4.2.2 Trivalent Cation Effect: Iron and Aluminum 49

4.2.3 Model to Predict Friction Reduction based on Water Quality 50

Chapter 5: Conclusion and Future Work 56

5.1 Conclusion 56

5.2 Future Work 57

Nomenclature 57

List of Figures

Figure 1 -Flow Regimes in Turbulent Flow over a Flat Plate…….....7
Figure 2 - Laminar and Turbulent Flow Velocity Profile …….…….....8
Figure 3 - Qualitative Description of Friction Reduction.…….....10
Figure 4 - Development of the Velocity Boundary Layer in a Pipe …….....11
Figure 5 -Shearing Effect on Polymer Arrangement in Solution…….....13
Figure 6 -Experimental Results Plotted Against the Maximum Drag Reduction Asymptote ……...……..…….....17
Figure 7 -Polyelectrolyte Cation Interactions……...…….……..24
Figure 8 -Partially Hydrolyzed Polyacrylamide Structure…….....26
Figure 9 -Inversion Process of an Oil in Water Emulsion…….....28
Figure 10-Shale Water Research Center Friction Flow Loop…….34
Figure 11-Typical Successful Friction Reducer Performance Curve. 150 ppm of FR-A in low-TDS water…….....……35
Figure 12-Effect of Polymer Degree of Hydrolysis on Friction Reducer Performance. 1 gpt of 0-30% HPAM in SFW (3,000 mg/L) over time....37
Figure 13-Effect of Polymer Degree of Hydrolysis on Friction Reducer Performance. 1 gpt of 0-30% HPAM in SPW (120,000 mg/L) 38
Figure 14-Effects of Polymer Concentration on Friction Reduction. 0.0003 gpt-2 gpt 30% HPAM in Low-TDS Water Over Time...….....39
Figure 15-Friction Reduction of 1 gpt 30% HPAM in Synthetic Produced Waters from 3,000-120,000 mg/L……..……...……40
Figure 16-Friction Reduction of 1 gpt 30% HPAM in NaCl Solutions of 3,000-120,000 mg/L……41
Figure 17-Friction Reduction of 1 gpt 30% HPAM in low-TDS water with 2,860 mg/L Mg2+ and 4,700 mg/L Ca2+ respectively……..……41
Figure 18a-Friction Reduction of 1 gpt FR-A in low-TDS water with the addition of 50 ppm Fe(III) solution and EDTA. …….....42
Figure 18b-Friction Reduction of 1 gpt FR-A in low-TDS water with the addition of 20 ppm Fe(III) solution and EDTA……..... 43
Figure 19-1 gpt of FR-A in low-TDS water with 50 ppm Fe (III) in a Beaker……...…….....43
Figure 20a-1 gpt of 30% HPAM in low-TDS water with 50 ppm Al(III). No friction reduction ……...……...43
Figure 20b-1 gpt of 30% HPAM in low TDS-water. Addition of 50 ppm Al(III) lowers friction reduction……43
Figure 21-1 gpt 30 % HPAM in low-TDS water with 50 ppm Al(III) in a Beaker…44
Figure 22-Viscosity of a Solution as a Function of Polymer Concentration …..…...45
Figure 23-Calcium and Polymer Bridging……...…….....47
Figure 24-Effect of ion-ion interactions on friction reducer performance. 1 gpt 30% HPAM in different water qualities……48
Figure 25- Fitted Exponential Decay Model to 1 gpt (300 ppm) 30% HPAM in SPW from 3,000 mg/L to 120,000 mg/L……....51

Figure 26 – Plot of Residual Values (%FR measured-% FR predicted) between model and experimental data from Fig. 25 as a function of time……52
Figure 27- Fitted Exponential Decay Model to 1 gpt (300 ppm) FR-A in Real Produced Water from 1,500 mg/L to 97,700 mg/L…….53
Figure 28 - Plot of Residual Values (%FR measured-% FR predicted) between model and experimental data from Fig. 28 as a function of time……54

List of Tables

Table 1-Produced Water Quality..…….……...……29
Table 2- Real and Synthetic Produced Water Compositions Used in Experiments..32
Table 3-Calculated and Measured Friction Reduction Degradation over Experimental Period in Synthetic and Real Produced Waters……..55

Chapter 1: Introduction

1.1 Problem Statement

Produced water reuse for hydraulic fracturing has become increasingly important in the oil and gas industry due to more stringent disposal regulations, limited freshwater availability, and high water treatment costs. The incompatibility of fracturing fluids with the high concentrations of dissolved ions in produced water has made water reusing extremely challenging for the industry. Decreased friction reducer performance in slickwater fracturing has been one of the major problems associated with produced water reuse. The effectiveness of these long-chained polymers is critical to economically achieve the fast pumping rates required for slickwater fracturing. Friction reducer (FR) performance can be completely degraded in highly incompatible water, and increase pumping pressures to prohibitive levels. In the presence of trivalent cations such as Fe^{3+} and Al^{3+} friction reducers can sometimes flocculate out of solution as gel precipitates. These gel precipitates have shown to cause formation damage that lower production rates, and make it more difficult for the well to be cleaned out. Without friction reducers, the slickwater operation would not economically feasible.

Preventing unwanted friction reducer interactions is crucial to ensure a successful slickwater hydraulic fracturing operation. Predicting friction reducer performance in different conditions has been difficult because it combines two areas in science that are

still poorly understood: turbulence and polymer behavior in solution. As a result, the effects that specific ions and waters will have on performance are largely unknown in the industry. This lack of understanding has led to extremely high water treatment costs to remove all of the impurities that might have an effect on the polymer, and to uncertainty in the field when friction reducer operational problems arise. There is a need for a characterization of friction reducer behavior in brines in order to be able to choose the right friction reducer, and water treatment technology for each operation.

1.2 Purpose of the study

The purpose of this study is to characterize the behavior of friction reducers in field conditions as a function of polymer, and water characteristics. Most of the research focusing on this problem has only published experiments on friction reduction in NaCl or tap water solutions (Shah and Kamel 2010) (Paktinat, O'Neil, et al. 2011) (Zhou, Sun and Qu 2011). The little work that has been done on complex brines that resemble produced water has not disclosed information about the compositions of the friction reducers and is therefore not very applicable. (Ferguson and Johnson 2009) (Zhou, Sun and Qu 2011) (C. Aften 2010) Detailed theoretical and experimental work has been done on specific ion-polymer interactions but is of little use for application purposes because it does not tie these interactions to to friction reducer performance. Until a theoretical model can be developed, a characterization of friction reducer behavior from experimental results is needed. In this work, partially hydrolyzed polyacrylamide, the most commonly used friction reducer, is tested in a friction flow loop as a function of degree of hydrolysis (0-30%), and concentration, in different synthetic produced water qualities. The effects of NaCl, $Ca^{2+,}$ $Mg^{2+,}$ Fe^{3+}, and Al^{3+} on friction reduction are

individually examined. Finally, an empirical equation to predict friction reduction based on produced water TDS is proposed. The equation is tested and validated with performance results of a commercial friction reducer in real produced waters.

The theoretical background and literature review on friction reduction will be covered in the next chapter. Chapter 3 will cover materials and methods, and the experimental details of the friction reducers and waters tested. The results, and discussion will be presented in Chapter 5. Finally, Chapter 6 will include the conclusion and future work.

Chapter 2: Background and Literature Review

2.1 Introduction to Friction Reducers

Friction reducers (also known as drag reducers) are high molecular weight polymers that added at low concentrations can reduce frictional energy dissipation in turbulent flows up to 80% (Aften and Watson 2009). By conserving this energy, faster flow rates are achieved at the same pumping pressure than by using the solvent alone. These polymers are added to water and proppant in slickwater hydraulic fracturing to fracture the formation. Slickwater hydraulic fracturing has been rapidly replacing conventional gel fractures due to its low chemical cost and ease of well cleanup. In order to make up for the low viscosity of the slickwater, low concentration of friction reducers (300-2600 ppm) are used to achieve high flow rates (60-120 bbls/min), and ensure effective formation fracturing. Low FR performance in the field causes a spike in pumping pressure for a given flow rate and if sustained could ruin the entire operation.

The most commonly used friction reducers in hydraulic fracturing are polyacrylamide and acrylic acid copolymers of around 20-30% acrylic acid, and of a molecular weight range of 5-30 million Dalton(Hoyt and Wade 1973). In terms of effectiveness (concentration needed for a given degree of friction reduction), polyacrylamide lies between guar and poly (ethylene oxide) but it is more widely used because it dissolves more readily in water(Hoyt and Wade 1973). The FR is usually in a water-in-oil emulsion form that releases the polymer into the solution by a process termed “inversion” creating an oil-in-water emulsion after addition. The inverse emulsion form makes it easier to pump, disperse, and hydrate the polymer (Carman and K.E. 2007) but for transportation

and storage convenience, the powder form of the polymer has also been used. Polymer dosage ranges between 0.25-2 gallons of polymer per 1000 gallons of water (0.25-2 gpt) or 75-2000 ppm active polymer depending on the percentage of friction reducer in the inverse emulsion solution.

2.2 Friction Reduction Mechanism

2.2.1 General Conclusions from the Literature

Polymeric friction reduction was accidentally discovered by Toms in 1947 who observed that adding parts per million of polymethylmethacrylate to monochlorobenzene could significantly reduce the pressure drop experienced during turbulent flow (Lumley 1969) (McAllister 2009). Since then, this phenomenon has been known across the literature as "the Toms effect" and has been proven to apply to dilute solutions of linear long-chained polymers in turbulent flows.

The ability to considerably reduce frictional energy dissipation has been used in many industries to efficiently increase flow rate and maintain moderate pumping pressures. Poly(ethylene)oxide is used to increase foam spreading in firefighting (Schramm 2013), long-chain hydrocarbons are used to increase flow rates in oil pipelines, and other polymers are used to prevent overflow during increased sewage output, among their many applications. The use of polyacrylamide-based friction reducers has been vital to the shale boom because it has allowed for production of shale formations that would be otherwise too expensive.

Despite the widespread application and the extensive research done on FRs, the mechanism of friction reduction remains poorly understood. Even the most recent advanced numerical simulations cannot seem to capture the complexity of the process. This is a consequence of the fact that neither turbulent flow nor polymer behavior in solutions has been yet fully explained. (Sreenivasan and White 2000). Nonetheless, the vast number of research experiments have shed some light into the details of the mechanisms, and provided a generally accepted qualitative view of the process.

Notable advances were made by Toms in 1948 [59]who made the discovery, Hoyt and Fabula in 1964 [28] who showed that long linear polymers with minimum chain branching were ideal for friction reduction, Virk in 1975 [63] who proposed a mechanism and discovered the maximum drag reducing asymptote, Merril et al (1966) [39]showed the importance of chain length on friction reduction, and experiments by Hershey and Zakin (1967) in different solvents showed that friction reduction increased in good solvents and must be related to polymer chain expansion. Lumley's review paper [37] provides a good summary of all of the relevant experimental evidence published before 1969. More recent research papers have focused on the behavior of the polymer in solutions of different brines [4][42] but either do not incorporate conditions similar to the field, or do not disclose enough information making it difficult to make any significant conclusions from the results. Researches on polymer adsorption onto colloidal surfaces and polyelectrolyte studies have been able to partially describe the coiling effect that ions in brines can have on friction reducers. This has shed some light on the mechanisms of polymer crosslinking and bridging, but the relationship to friction reducer performance is

still lacking. Nevertheless, a predictive tool is still desperately needed in the industry. Given that the theoretical groundwork has not been completely paved in matters of turbulence or polymer research, an empirical formulation is currently the most applicable route to pursue.

2.2.2 Fluid Mechanics

2.2.2.1 Laminar and Turbulent Flow Profiles

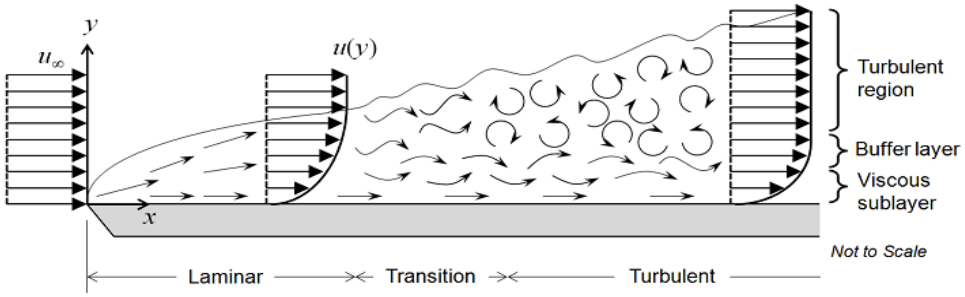

Figure 1-Flow Regimes in Turbulent Flow over a Flat Plate [8]

When a fluid flows over a surface, a velocity profile is created. By the wall, the adhesive forces of the fluid molecules onto the solid surface are stronger than the cohesive forces to the rest of the fluid, and the velocity of the fluid is zero. This effect is known as the no-slip condition and is responsible for the velocity and turbulence profile shown in Fig. 1 and Fig. 2. (Fitzpatrick 2012). If the average velocity is low enough or the surface of the wall is really smooth, the fluid molecules above the wall flow in an orderly manner and are called laminar flow as shown in the first section of Fig.1. In laminar pipe flow there is a parabolic velocity distribution shown in Fig 2 where the velocity gradually increases

from zero at the wall to a maximum value at the center of the pipe. In this flow, the layers of fluid slide over each other linearly and the velocity perpendicular to the flow is zero. When the fluid velocity increases, laminar flow begins to have a perpendicular component known as the transition region until a fully turbulent core develops in the pipe. Turbulent flow is highly chaotic, characterized by turbulent eddies that dissipate energy from the fluid. The velocity profile is no longer smooth one-dimensional flow as in the case of laminar flow, but is rather chaotically fluctuating in three dimensions with time. This results in much higher energy consumption for a certain average velocity than smooth laminar flow, and is reflected in the high power required to pump turbulent flow at high velocities. Near the wall, the velocity is low enough due to the no-slip condition that a laminar viscous sublayer is always present. As the fluid velocity increases further away from the wall, a buffer layer is exists where flow conditions exhibit both laminar and turbulent characteristics. Much of the mixing characteristic of turbulent flow is promoted by stream-wise vortices called streaks that are generated intermittently near the wall. These vortices rapidly grow and decay in the buffer layer causing the chaotic conditions in the turbulent core. The development of the turbulent streaks is characterized by a triggering mechanism such as the unsteady flow structures that develop naturally, surface

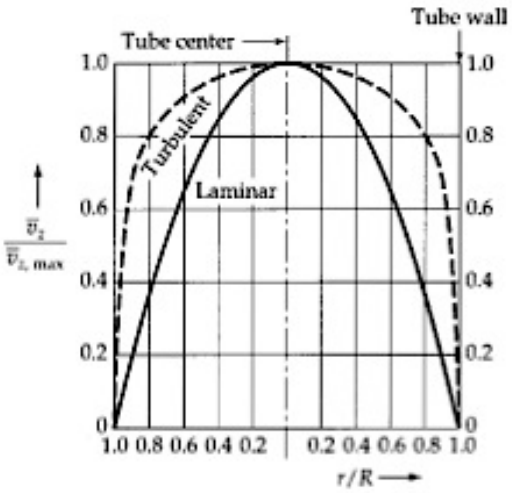

Figure 2- Laminar and Turbulent Flow Velocity Profile in a Pipe [9]

roughness, or vibrations (Bird, Stewart and Lightfoot 2006).Friction reducers are thought to interact with the eddy triggering mechanism and reduce it.

2.2.2.2 Qualitative Mechanism of Friction Reduction

The chaotic nature of turbulence has made it impossible to derive a quantitative theory that encompasses the non-linear equations that govern it. Experimental and analytical results have shown that friction reducers interact with the turbulence eddies but the lack of a theory to describe the flow has made it impossible to quantitatively characterize the behavior of the polymers in solution. It is generally accepted, however, that molecular flexibility, linearity, high molecular weight, and good solvent interactions are the most important parameters in friction reduction of polymer solutions (Ting and Kim 1973). Direct numerical simulation has made significant advances to model turbulent flow in recent years, however due to the large computational efforts required, it has remained restricted to slow flows, simple geometries, and Newtonian fluids. Most theories and experimental results are some form of the theory proposed by Virk in 1975 [10,27,37,39,63]. He postulated that the addition of friction reducers interfered with the turbulent bursts in the buffer layer increasing the distance from the wall beyond which the flow is turbulent (Virk 1975) (Lumley 1969). This results in an effective thickening of the buffer layer (which he called an elastic sublayer) that contains a laminar and turbulent component. At theoretical maximum friction reduction, Virk envisioned the elastic sublayer completely filling the turbulent core. Fig. 3 shows the turbulent bursts in the buffer region before the addition of the friction reducer and after the addition of the friction reducer. The polymer is thought to serve as a burst shock absorbent and prevent eddy propagation. A high molecular weight linear polymer is the most effective at

friction reduction because it can stretch out and have the maximum interactions with the eddies . After the addition of the polymer, the turbulent core becomes much more like the buffer region, and frictional energy losses are reduced.

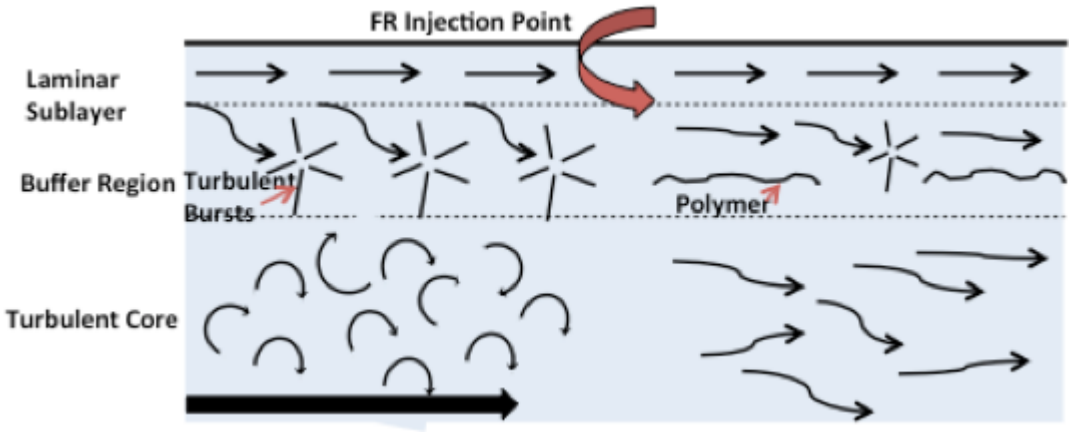

Figure 3-Qualitative Description of Friction Reduction in a Pipe

Other prominent theories hypothesize that the mechanism involved is not turbulence dissipation but rather a reduced production of turbulence [23] or that the friction reducer stores energy changing the structure of turbulence[64,29]. However, this area remains in active discussion and no definitive conclusions have been drawn.

2.2.2.3 Reynolds Number

A dimensionless parameter was developed to calculate the transition from turbulent to laminar flow called the Reynolds number, Re. It is a ratio of the viscous forces to the inertial forces in flow. When viscous forces are dominant, then the fluid can suppress the formation of turbulent eddies and the flow is laminar. When inertial forces dominate then turbulent eddies are created at the sublayer, and a turbulent core develops. Eq. 1 shows that the Re is proportional to the linear velocity, and pipe diameter (inertial forces) and decreases with increasing viscosity (viscous forces).

$$Re = \frac{inertial\ forces}{viscous\ forces} = \frac{u_{avg}L_c}{v} = \frac{\rho u_{avg}L_c}{\mu} \quad (1)$$

Experimental values report that the transition between laminar and turbulent flow occurs between 2100 and 4000. This range is known as the critical Re but the exact value depends on velocity, surface roughness, and fluid properties.

2.2.2.4 Hydrodynamic Entrance Length

When fluid enters a pipe and encounters the no-slip condition, the velocity profile takes time to fully develop into the laminar parabolic shape or the time-averaged turbulent shape shown in Fig.2. The distance required for the flow to fully develop is known as the hydrodynamic entrance length, $L_{h,}$ and is an important value to know when studying flow through pipes. The distance can be approximated in laminar flow by Eq. 2 and in turbulent flow by Eq. 3. Intense mixing in turbulent flow decreases the entrance length and the equation shows that it is less dependent on the Re than the laminar hydrodynamic length is. For most engineering interests the length can be approximated as 10 times the pipe diameter(Cengel and Cimbala 2010).

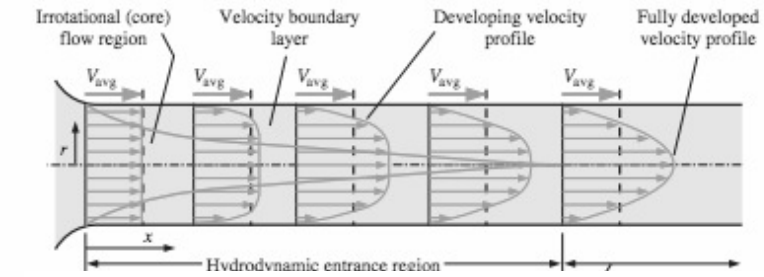

Figure 4- Development of the Velocity Boundary Layer in a Pipe [14]

$$L_{h,laminar} = 0.05ReD \quad (2)$$

$$L_{h,turbulent} = 1.359DRe_D^{1/4} \sim 10D \text{ (for most engineering interests)} \quad (3)$$

2.2.2.5 Shear Rate and Shear Stress

Shear strain rate and shear stress are a measure of the force applied to fluid in the direction of flow. Stress, τ, refers to the force per unit area applied on the fluid. Strain is a measure of the relative change in length as a result of the applied stress. The rate of straining $d\Upsilon/dt$ is related to stress (in Newtonian fluids) through a proportionality constant called viscosity. Viscosity is a measure of the fluid's resistance to stress. Shear stress rate can be calculated for a Newtonian fluid in a pipe with Eq. 4

$$\dot{\gamma} = \frac{d\gamma}{dt} = \frac{8u}{D} \tag{4}$$

Shear refers to the direction of the force being parallel to the plane. These two parameters are used to describe the mechanical forces that affect friction reducers and fluids when flowing through pipes.

2.2.2.6 Friction Factor

The friction factor is the ratio of shear stress to the dynamic pressure of the fluid (kinetic energy per unit volume). Friction refers to the force that resists motion and thus causes energy losses during flow. Friction reducers act by decreasing the resistance to flow and thereby conserving energy.

$$f_D = \frac{2\tau}{\rho v^2} \tag{5}$$

The Darcy friction factor (above) is sometimes confused with the fanning friction factor, $f_r = f_D/4$. For laminar flow in Eq. 6, the friction factor only depends on Re and not on surface roughness.

$$f_D = \frac{64}{Re} \text{ (laminar flow)} \tag{6}$$

$$\frac{1}{\sqrt{f}} = -2.0 \log\left(\frac{\varepsilon}{3.7D} + \frac{2.51}{Re\sqrt{f}}\right) \text{(turbulent flow)} \quad (7)$$

For turbulent flow, the friction factor (energy lost) is a function of both the Re and the roughness of the pipe, ε. However, the equation for this dependence cannot be derived from theory and the only relationships available are from experimental data (Cengel and Cimbala 2010). The Colebrook equation (Eq. 7)is an implicit approximation that can be used to estimate the friction factor in turbulent flow. The Moody Chart (Appendix) is most commonly used for this purpose giving the friction factor as a function of roughness and Re.

2.2.2.7 Viscoelasticity and Non-Newtonian Behavior

Newtonian fluids, such as water, are fluids that exhibit a constant resistance to flow (viscosity) independent of the shear strain applied to it. Dilute polymer solutions, on the other hand, are non-Newtonian solutions that have a shear stress dependent viscosity. For these solutions, viscosity decreases as shear stress increases, and are known as non-Newtonian shear thinning fluids. Shear thinning behavior is a result of the viscoelastic component that the polymers provide the solution. These solutions have the viscous component from a traditional Newtonian fluid, but the long polymers in solution also supply an elastic response to shear stress such as that from a it Hookean spring. Fig. 5 shows a qualitative view of shear-thinning behavior. At low shear rates, the polymers are coiled, and randomly arranged in the solution. As the shear rate increases, the force causes the

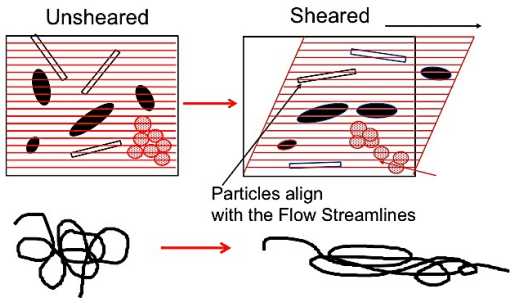

Figure 5-Shearing Effect on Polymer Arrangement in Solution[69]

polymers to begin to uncoil and arrange themselves with the streamlines. This arrangement causes less resistance to flow, lowering the viscosity of the solution. As expected, modeling the behavior of non-Newtonian solutions is much more difficult than that of ideal Newtonian solutions.

Some of the most commonly used models to describe the shear stress and strain relationships for non-Newtonian fluids are modeling the behavior with: Bingham Plastic equation, a power law model where K is the consistency index and $n<1$ is the power law exponent, the Casson Model, and the Herschel-Buckley Model, Eq. 8-11 respectively.

$$\tau=\tau_y+\mu_\infty \gamma \quad (8)$$

$$\tau=K\gamma^n , \mu=K \gamma^{n-1} \quad (9)$$

$$\tau=\tau_0^{0.5}+\mu_\infty^{0.5} \gamma^{0.5} \quad (10)$$

$$\tau=\tau_0+K\gamma^n \quad (11)$$

Friction reducers usually fit the power law equation well, and some of the K and n parameters can be found reported in the literature from experimental results.

2.2.3 Characteristics of Friction Reducing Flow

2.2.3.1 Onset of friction reduction

An onset of friction reduction has been observed to occur for dilute polymer solutions. Below a certain flow rate for a given system, the polymer solution and the solvent behave the same. Once the flow rate is increased, the frictional dissipation of the polymer solution begins to decrease (Virk 1975). The amount of friction reduction increases with flow rate until a maximum value is finally achieved. This value would be theoretically

sustained by the solution at higher and higher flow rates if the increasing shear stresses did not begin to degrade the polymer. The effect of the polymer on friction is evaluated by comparing the friction factors of both solutions at the same conditions. Experiments studying friction reduction in systems of different pipe diameters showed that the onset of drag reduction for a given polymer depends on shear rate and not Re as is sometimes thought (Virk 1975). In poor solvents, the onset of drag reduction is delayed due to the interactions of the solvent with the friction reducer.

2.2.3.2 Molecular Weight and Linearity of the Polymeric Friction Reducer

Polymer molecular weight is a determining parameter for friction reduction[53]. The longer the polymer chain, the more it can interact with the bursts of turbulent eddies and provide more friction reduction. Linear molecules perform better as friction reducer because branching increases the turbulence caused by the flow of the molecules, and does not adsorb the shock of the turbulent eddies as well as the linear molecules do. Average molecular weights used in the field for friction reducers are 5-30 million Dalton of linear friction reducer. Higher molecular weight becomes too susceptible to shear degradation, and to crosslinking with other polymers in solution so they are not usually chosen (Caruso, et al. 2009).

2.2.3.4 Virk's Maximum Drag reduction asymptote

Virk's 1975 [63]famous paper described an asymptote of maximum friction reduction that could be calculated for any system. The paper defined three flow regimes for dilute polymer solutions in turbulent flow. The first regime was characterized by the Prandlt-Karman law for Newtonian turbulent flow, Eq. 7 (an earlier version of Eq. 6), in which

the polymer solution was expected to behave like the solvent solution and the friction factor was only dependent on Re. The second regime Eq. 8, is the regime in which the onset of friction reduction has occurred, and the friction factor depends on the Re and δ, W^0(polymer-specific parameters). The third regime is where the elastic boundary layer has fully expanded into the turbulent core and maximum drag reduction has been obtained. This regime, Eq. 9, is independent of pipe diameter, polymer species, molecular weight, and concentration. Fig. 6 shows the fit to the experimental results.

$$f^{-\frac{1}{2}} = 4.0 \log_{10} Re\, f^{1.2} - 0.4 \tag{7}$$

$$f^{-\frac{1}{2}} = (4.0 + \delta) \log_{10} Re\, f^{\frac{1}{2}} - 0.4 - \delta \log_{10} \sqrt{2}\, dW^0 \tag{8}$$

$$f^{1/2} = 19. \log_{10} Re\, f^{1/2} - 32 \tag{9}$$

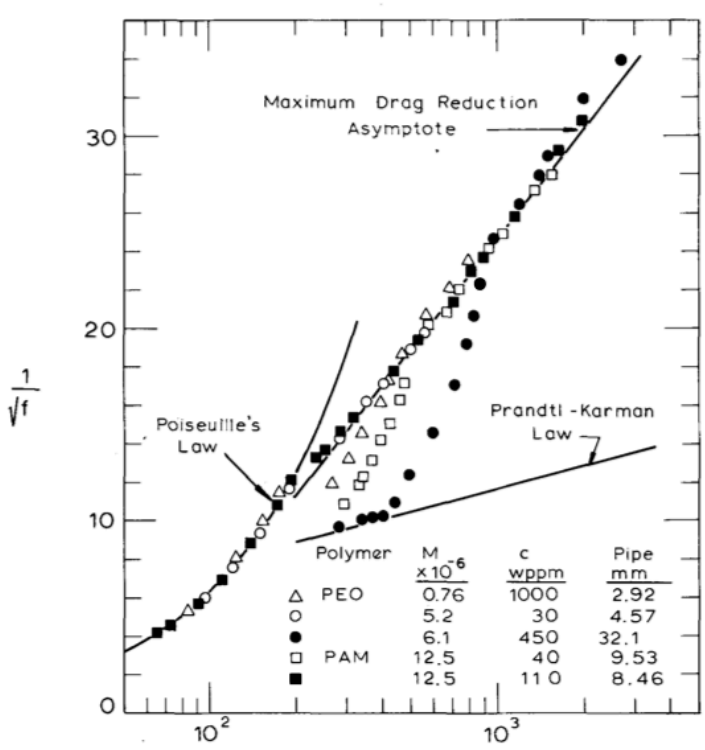

Figure 6-Experimental Results Plotted Against the Maximum Drag Reduction Asymptote [63]

At low Re, the polymers follow poiseulle's law for laminar flow(Eq. 6), then, as flow rate increases, the solutions follow the Prandlt-Karman law for turbulent Newtonian fluid. At higher flow rates the curve deviates into the non-Newtonian regime of friction reduction towards the maximum drag

reduction asymptotes. The biggest significance of the maximum drag reduction asymptote is that all dilute polymer system, regardless of polymer type, can theoretically achieve maximum friction reduction in the right conditions. Most friction reducing solutions, however, lie somewhere between the Prandlt-Karman law and the maximum drag reduction asymptote.

2.2.3.5 Extensional Viscosity Effects

Extensional viscosity effects have been used by rheologists to explain friction reduction. Analogous to shear viscosity, extensional or elongational viscosity is a measure of the resistance of the polymer to elongational stresses. Elongational viscosity measurements have shown that in shear stress, dilute polymer solutions experience a dramatic increase in this viscosity. Shear viscosity, on the other hand, decreases only slightly usually remaining close to the solvent viscosity. The increase of extensional viscosity manifests itself near the wall where the extensional strain rates are the highest, and has been measured to increase by 3 decimal places in dilute polymer solutions. Increased local polymer viscosity can suppress turbulence dissipation and be responsible for drag reduction. A Zimm-bead spring model, Eq. 10, has been used to describe the elongational viscosity effect.

$$\eta = 3\eta_0[1 + 2C[\eta]N + \cdots] \tag{10}$$

Experimental evidence has shown that there is a strong correlation between N, and [η] with friction reduction, further supporting evidence between the correlation of elongational viscosity and drag reduction (Cowan, et al. 2000). However, no experiments

have been able to directly measure this correlation, and the parameters used to make the correlation are polymer properties that simultaneously support the boundary-layer theory.

2.2.3.6 Dilute Solutions and Critical Overlap Concentration

Flexible polymers are in a random coiled state in solution. Effective friction reduction is related to the ability of the polymer to uncoil and interfere with turbulence bursts. Increasing polymer-solvent interactions for higher polymer expansion is necessary for good friction reduction. Good polymer-solvent interactions (theta solvents) increase the contact of solvent molecules with polymer segments, and lead to larger hydrodynamic volumes, polymer uncoiling, and friction reduction. Charged groups on the polymer chain also provide an increased hydrodynamic volume as a result of electrostatic repulsion. When polymer-polymer interactions are favored over polymer-solvent interactions, polymer coiling and entanglement prevent the polymer from interfering with the turbulent eddies and acting as effective friction reducers. The critical overlap concentration is defined as the concentration at which the solution can no longer be considered dilute and polymer-polymer interactions begin to become more relevant than polymer-solvent interactions.

One of the earliest theories for polymer solution behavior is the Flory-Huggins equation. The Flory-Huggins theory predicts the free energy of mixing, ΔG_{mix}, for polymer-solvent mixtures by using a lattice model. Each lattice cell is occupied by a segment of polymer or a solvent molecule where the polymer segment volume equals that of the solvent molecule. The ratio of molar volumes $\frac{V_{polymer}}{V_{solvent}} = \sigma$ is a measure of the volume occupied by the polymer relative to that of a solvent molecule. ΔG_{mix} is a function of the

number of possible spatial configurations of the connected polymer segments in the lattice. The Flory-Huggins interaction parameter Eq. 11 accounts for the polymer interactions by considering the z number of contact points of the molecule and the polymer solvent interaction energies $\mathbf{\Delta w_{12}}$ (Chanda 2000).

$$\chi_{12} = z\Delta w_{12}/kT \quad (11)$$

$$\Delta G_{mix} = -R[n_1 \ln \Phi_1 + n_2 \ln \Phi_2 + n_1 \Phi_2 \chi_{12}] \quad (12)$$

where $\Phi_1 = \frac{N_1}{N_1 + \sigma N_2}$ $\Phi_2 = \frac{\sigma N_2}{N_1 + \sigma N_2}$

Combining these concepts yields the Flory Huggins model, eq. 12, where and N_1, N_2 represent the number of solvent and polymer molecules respectively. This equation accounts for the equilibrium thermodynamic properties of the solution but has its limitations particularly when the polymer solution has a dilute concentration. In dilute solutions large regions of solvent alone isolate the polymer molecules but the lattice model assumes that the polymer segments are uniformly distributed in the lattice. This model also fails for polyelectrolytes , excluding important inter and intra molecular electrostatic interactions. The Flory-Krigbaum theory, a modification of the Flory Huggins model, views polymer concentration within an elemental volume and can in that way be applied to dilute polymer solutions. The critical polymer overlap concentration can be calculated using this model by means of Eq. 13 .

$$c_{overlap} = \frac{1}{0.16\sqrt{M}} \quad (13)$$

The dilute nature of the solutions that exhibit drag reduction and the decrease in friction reduction past the critical overlap concentration suggests that individual molecules are involved with the drag reduction process rather than entangled clusters. This

concentration is dependent on the solvent and polymer type, and polymer molecular weight

2.3 Polymer Degradation Mechanisms

2.3.1 Importance of polymer coil size, ionic groups, and linearity

Polymer degradation causes friction reducer performance to decrease in certain solutions. In order for a polymer to perform well as a friction reducer, it must be an uncoiled, linear, high molecular weight polymer. Anything that affects these parameters has an effect on friction reduction. Polymer "scissoring" or bond breaking of the molecule occurs because of high shear rate that physically scissors the polymer or because of radical chain degradation that chemically scissors the polymer. Linearity and coiling is affected by the presence of ionic agents that electrostatically reduce the radius of gyration of the polymer and sometime crosslink it with other polymers creating a non-linear network. The importance of linear polymer uncoiling and stretching has been emphasized in all related publications [2,4,6,9,10]. Evidence supports the importance of strong solvent-polymer interactions to promote friction reduction. In good solvents, the polymers take on an expanded conformation because polymer-contact solvents are favored and in poor solvents a more compact conformation where polymer -polymer interactions are favored(Hershey and Zakin 1967).

2.3.2 Shear Degradation Mechanisms

Polymer scission from shear stress occurs above a critical elongational stress. This scission has been shown by GC, and elongational viscosity experiments to occur as a Gaussian distribution in the midpoint of the polymer (Kim and Choi 1996). Higher

polymer length and chain flexibility are increasingly susceptible to shear degradation (Hunston and Zakin 1978). The polymer scission occurs in extensional flows where the shear rate uncoils the polymer and stretches it to a "fully extended state" for a period of time. Tension distributes itself parabolically so that the maximum is at the center of the polymer where the scission is more likely to occur. Models predict that the critical strain rate that causes scission is inversely proportional to viscosity and to molecular weight squared (Sim 2007). Chain rigidity also provides the polymer more resistance to shear degradation. Polyacrylic acid is a shear stable polymer due to its rigid nature compared to flexible polyethylene oxide and polyacrylamide, which have good friction reducer capabilities. Polyacrylic acid and polyacrylamide copolymers have moderately good shear stability and good friction reduction as a result of these characteristics.

Shear rate increases with velocity and decreases with diameter (Eq. 4). Thus, shear degradation becomes important in small diameter tubing, extremely high flow rates, or when flowing through pumps because the shear stresses are larger. As a result of this, friction reducers are sometimes added after the pump to prevent shear degradation(Kim and Choi 1996).

2.3.3 Radical Chain Degradation

Free radicals in solution, particularly from metal salts or oxidative agents, have been linked to a chemical polymer chain degradation mechanism that results in shorter polymer molecules. Breakers used to detach the friction reducer from the formation after the fracking operation are conventionally oxidizers that operate under the radical chain degradation mechanism. The high concentration of free radicals in some recycled

produced waters has prematurely caused degradation of the polymer and negatively impacted friction reducer performance. Low iron concentrations have shown to have detrimental effects on the performance of the polymer. A proposed degradation mechanism leads to polymer fragments from the oxidation of iron (Ramsden and McKay 1986) (Carman P.S.l Cawiezel 2007):

$$Fe^{2+} + H_2O_2 \rightarrow Fe^{3+} + \cdot OH + OH^-$$
$$Fe^{2+} + \cdot OH \rightarrow Fe^{3+} + OH^-$$
$$PH + \cdot OH \rightarrow P\cdot + H_2O$$
$$P\cdot + O_2 \rightarrow PO_2\cdot$$
$$2PO_2\cdot \rightarrow P - O - O - O - O - P$$
$$P - O - O - O - O - P \rightarrow 2PO\cdot + O_2$$
$$PO\cdot \rightarrow F\cdot + F$$

Where P is the polymer, PH is the polymer with the removable hydrogen, F is the polymer fragment, and F· is the fragment radical. Chlorine dioxide, a common breaker, uses a similar free radical mechanism. The catalytic effect of iron oxidation on chain scissoring has a detrimental effect on friction reducer performance.

2.3.4 Monovalent Cation Electrostatic Effect on Radius of Gyration

Polyelectrolytes, as are most polymeric friction reducers, are affected by electrostatic interactions from charges around the molecule and on the molecule itself. The negative charges on the most commonly used friction reducer, partially hydrolyzed anionic polyacrylamide (HPAM), give it better friction reduction capabilities because the electrostatic repulsion of the negative charges on the molecule forces the polymer to uncoil more than it would without the presence of the charges. When the water solution has a high electrolyte concentration, however, the cations in solution shield the negative

charges of the polymer, screening the electrostatic interaction and reducing the polyelectrolyte friction reducer effect.

There are two important length parameters that are used when discussing discrete electrostatic interactions in polyelectrolyte solutions. The Bjerrum length, l_B

$$l_B = \frac{e^2}{4\pi\varepsilon kT} \tag{12}$$

is the length scale below which the Columbic electrostatic interactions between two charges are more important than the randomizing effects of thermal energy. This quantity needs to be considered when looking at close interactions between ions and charged monomers on the polyelectrolyte, particularly counter ion condensation (Adachi 2013) (Bazant 2011).

$$\kappa^{-1} = \sqrt{\frac{\varepsilon kT}{\sum_i e^2 n_{i_0} z_i}} \tag{13}$$

The Debye length, Eq. 13, determines the thickness of the electrical double layer which is effectively the length of electrostatic effect of a charge in solution. (Wikipedia 2014).

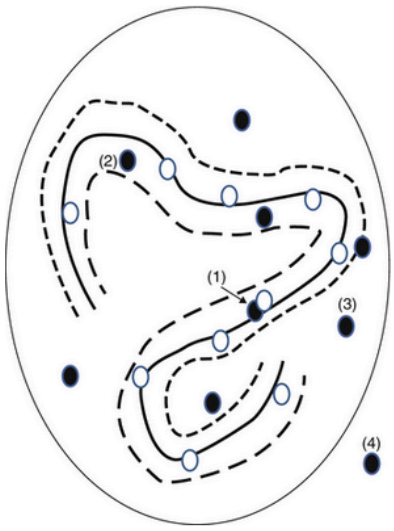

Figure 7-Polyelectrolyte Cation Interactions[4]

When cations are surrounding a negatively charged friction reducer, there is a screening of the negative charge and the Debye length is a measure of that screening. When looking at a charged polyelectrolyte such as the

one in Fig 7, counter ions (represented by the black circles) can either "(1) form an ion pair with the charge on the chain, (2) be present in the potential valley along the chain (3) be located in the region apparently occupied by the polyelectrolyte as a whole, and (4) be located outside the domain as a free ion. (Adachi 2013) ". When the solution has a high ionic strength such as produced water or seawater, the electrostatic shielding of the counter ions reduces the electrostatic repulsion of the charges on the polymer that cause it to expand and the chain shrinks (Fig. 7). Charge shielding and subsequent polymer coiling decreases friction reduction performance and is the primary method by which monovalent cations affect friction reducers.

2.3.5 Crosslinking and Hydrogen Bonding with Multivalent Cations

Counter ion condensation, ion pair formation, bridging, crosslinking, and hydrogen bonding are some of the terms used to describe the interactions of multivalent cations in solution with polyelectrolytes. When single counter ion or small charged particle interacts with the polymer, crosslinking between two different segments of the polymer can cause the polymer to coil. This is primarily important with divalent cations, where the higher charge causes the polymer to intra or intermolecularly crosslink. The same is true for trivalent cations except most of the ones found in produced water and in the formation (iron, aluminum) tend to be highly insoluble in water and instead exist as small colloidal hydroxides in solution to which the polymer can adsorb onto. When a polymer adsorbs onto more than one particle simultaneously, then this process is known as bridging. Most of the theory derived for polymer adsorption was made using a homopolymer (uncharged). The interaction of the charged tails, and surface charge has to be taken into account for polyelectrolytes. Adsorption of an oppositely charged polymer onto a

colloidal surface will cause the charge of the colloid to reduce until the charge is neutralized and flocculation occurs. Further polyelectrolyte adsorption could even lead to charge reversal of the colloid particle. When flocculation occurs then the polymer can no longer reduce friction and can additionally cause formation damage.

2.4 Slickwater Hydraulic Fracturing

2.4.1 Introduction to Slickwater Fracturing

Slickwater hydraulic fracturing is a method of hydraulic fracturing where water and proppant are mixed with a small amount of chemical to fracture the formation. Unlike conventional gel fractures, it has much lower chemical loading, yielding lower chemical costs. Additionally, the lower chemical loading allows for cheaper, faster, and easier well cleanup, which leads to less formation damage. These properties have made it the fracturing method of choice when possible(Kaufman, Penny and Paktinat 2008). However, low chemical loading translates to lower viscosity of the solution. Therefore slickwater hydraulic fracturing requires much higher pump rates to carry the proppant and effectively fracture the formation. Typical slickwater fracturing jobs pump water into the formation at around 100 bbls/ min whereas gel fractures usually do not exceed 60 bbls/min. In order to overcome these high pumping requirements, small concentrations of friction reducers are added to make the process economical and reduce pumping costs. Without the addition of friction reducers, the slickwater operation would not be economically feasible.

2.4.2 Additives and Fracturing Process

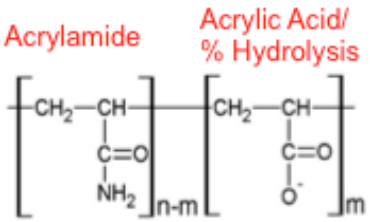

Figure 8-Partially Hydrolyzed Polyacrylamide Structure

The primary additive used in slickwater fracturing is the friction reducer. The most commonly used friction reducer is linear high molecular weight anionic polyacrylamide-based friction reducer, also known as partially hydrolyzed polyacrylamide (HPAM), but cationic and non-ionic copolymers have also been used. The anionic character of the HPAM is given by the acrylic acid group that hydrolyzes in water. The degree of hydrolysis of the polymer refers to the percentage of acrylic acid groups. The negative charges due to the degree of hydrolysis electrostatically repel each other and force the polymer into an expanded configuration, which increases its ability to reduce friction. Performance decrease in produced water is usually associated with interactions of cations in water with the acrylic acid group. Typical friction reducers used in the field range from 5-10 million Dalton and are around 20-30% hydrolyzed. To avoid polymer crosslinking and for faster dispersion in water, friction reducers are usually in a water-in-oil emulsion solution (inverse emulsion). They are sometimes also found in powder form when ease of transportation is necessary. Surfactants can be added with the friction reducer to speed up friction reducer solvation in the water. Dosages used in the field for maximum friction reduction range between 0.25-2 gallons of inverse emulsion friction reducer per 1000 gallons of water (gpt), which translates to 75-600 ppm active polymer in solution.

Despite the low concentration, friction reducers can interact with the salts in the water and rock and cause formation damage. Breakers are used after a fracking operation to

unclog the polymers from the formation. Oxidative agents such as persulfate and chlorine dioxide are usually employed to break the polymer backbone and increase polymer flowback. Understanding the formation and water composition is critical for adequate friction reducer selection.

Traditional fracking additives are also used in slickwater fracking. Biocides are added to prevent bacteria growth. Biocide-friction reducer interactions are important because opposing charges or free radicals in solutions can cause friction reducer degradation. Common biocides used are gluteraldehyde, and quarternary amines. Thione is relatively new but has shown to have no interaction with the friction reducer (Kaufman, Penny and Paktinat 2008). Scale Inhibitors are used to prevent scale formation. The most commonly used scale inhibitors are usually anionic and only provide major incompatibilities with cationic friction reducers. Clay stabilizers are sometimes used but the most commonly used is 2% KCl which interacts with the friction reducer and causes decreased performance.

2.4.3 Inverse Emulsions and the Process of Inversion

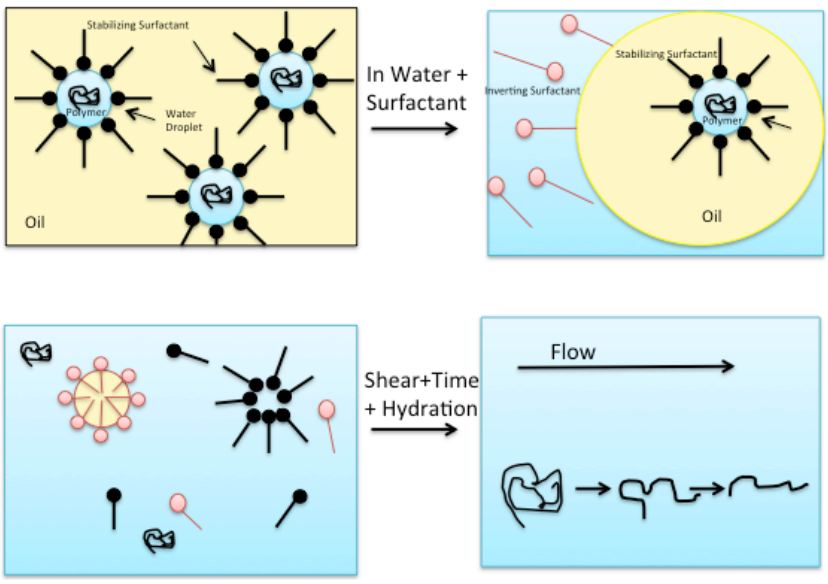

Figure 9-Inversion Process of an Oil in Water Emulsion

HPAM addition to water takes time to fully hydrate and enter the solution. Inversion refers to the process of hydrating the polymer in the water solution. For inverse emulsions this

refers to the polymer leaving the oil phase of the emulsion and entering the water fracking fluid phase. Fig. 9 shows the process of inversion for inverse emulsion friction reducers. First, the polymer is in water droplets dispersed in an oil phase stabilized by surfactants to prevent the polymer from crosslinking with other polymers in solution. When the friction reducer is added to water along with surfactant (not always necessary), the polymer leaves the water droplet in the oil phase and enters the water phase. The remaining oil in solution is then stabilized by the added surfactant into small oil droplets. Care must be taken in the field to ensure that a new batch of friction reducer is used since emulsions left to sit for too long can destabilize and the friction reducer crosslinks. Additionally, if no surfactant is added, lack of proper mixing could lead to reduced friction reducer performance.

2.4.4 Produced Water Composition

Produced water represents one of the major environmental concerns in the oil field. Currently produced water is handled by treatment and discharge into water sources, well injection, or treatment and reuse. Of those, reusing produced water is of great interest to the oil and gas industry. It represents a way to reduce the environmental footprint, maintain water in the water cycle, reduce transportation costs, and potentially reduce overall costs. The major challenge with produced water reuse is the interactions of the high metal concentration with oil-field chemicals. Relative to seawater, produced water has a high concentration of barium, iron, manganese, mercury, and zinc. (Neff, Lee and DeBlois 2011). There is also total organic carbon, organic acids, hydrocarbons, and production chemicals, but their interaction with friction reducers is still under investigation. In terms of total salinity, concentrations range from a few mg/L to over

300,000 mg/L. As shown by table 1, the water is usually composed of sodium and chloride ions but also has elevated calcium, magnesium, potassium, strontium, barium and aluminum concentrations . The study of the effect of iron on fracking additives has become important because, although there is a low concentration in solution, their effects have shown to ruin an entire operation. This work will use a range of produced water compositions that will attempt to capture the variety of ions present in produced water solutions.

Table 3-Produced Water Quality Table [41]

Parameter	Minimum value	Maximum value	Heavy metal	Minimum value (mg/l)	Maximum value (mg/l)
Density (kg/m^3)	1014	1140	Calcium	13	25 800
Conductivity (μS/cm)	4200	58 600	Sodium	132	97 000
Surface tension (dyn/cm)	43	78	Potassium	24	4300
pH	4.3	10	Magnesium	8	6000
TOC (mg/l)	0	1500	Iron	<0.1	100
TSS (mg/l)	1.2	1000	Aluminium	310	410
Total oil (IR; mg/l)	2	565	Boron	5	95
Volatile (BTX; mg/l)	0.39	35	Barium	1.3	650
Base/neutrals (mg/l)	—	<140	Cadmium	<0.005	0.2
Chloride (mg/l)	80	200 000	Copper	<0.02	1.5
Bicarbonate (mg/l)	77	3990	Chromium	0.02	1.1
Sulphate (mg/l)	<2	1650	Lithium	3	50
Ammoniacal nitrogen (mg/l)	10	300	Manganese	<0.004	175
Sulphite (mg/l)	—	10	Lead	0.002	8.8
Total polar (mg/L)	9.7	600	Strontium	0.02	1000
Higher acids (mg/l)	<1	63	Titanium	<0.01	0.7
Phenol (mg/l)	0.009	23	Zinc	0.01	35
Volatile fatty acids (mg/l)	2	4900	Arsenic	<0.005	0.3
			Mercury	<0.005	0.3
			Silver	<0.001	0.15
			Beryllium	<0.001	0.004

Chapter 3: Materials and Methods

3.1 Materials

3.1.1 Fracturing Additives

Inverse emulsion partially hydrolyzed polyacrylamide (HPAM) samples of 0%, 10%, 20%, and 30% carboxylic groups were supplied by Axchem and used as received. The active polymer concentrations in the solution were 32%, 32%, 39%, and 31.5 % respectively, and weight average molecular weight was of 10,000,000 Da. A commercial Ashland HPAM oil-field friction reducer, FR-A, was used to compare the purchased copolymers to a commercial friction reducer of similar composition. Concentrations tested range from 0.1-ppm active polymer concentration (volume added was adjusted for active concentration) to about 600-ppm active polymer concentration. Typical field values added are 0.25-2 gallons/1000 gallons of water so the concentrations tested fell within the ranges used in the field. Inverting surfactant, AP-SURF1, used in the field was added at a 1:1 concentration with the friction reducer to facilitate polymer demulsification in the water phase (Aften and Watson 2009). No other fracturing additives were added with the friction reducer. For the purposes of studying the interactions of friction reducer with the ions in the water, the effects of interactions with other additives was ignored.

3.1.2 Water Composition

The performance of the polymers was evaluated in waters of varying TDS and multivalent cation concentrations summarized in table 2. The U.S. Geological Survey National Produced Waters Geochemical Data Base[60] was used to determine the composition of the synthetic produced waters used for the experiments. An average of the

high-brine water samples (35,000-300,000 mg/L) was calculated from the database, and used for the synthetic produced water (SPW) values shown in table 1. The 120,000-mg/L synthetic produced water calculated from the database was diluted to 60,000 and 30,000 mg/L with the addition of deionized water and was also used for the experiments. This was done to reflect friction reducer performance in lower TDS produced waters as well as in produced waters that are diluted to lower concentrations in the field. Shale Water Research Center's database of river and pond water used in fracking operations was used to determine an average composition of "fresh water" that is used in the field. The Low-TDS water listed in the table is an average of the tap water compositions that were measured and used in the experiments. This water is expected to have the highest friction reducer performance due to its low ion concentration. Deionized water was not used for the low TDS water because the lowest-TDS water that would ever be used in the field is tap water, and because polyelectrolyte behavior in zero ionic strength water is drastically different than would ever be experienced. The pH of the analog produced waters was controlled by the addition of 10 mM PIPES buffer, but experiments showed that there was not much performance variation between pH of 3-9.

For comparison purposes and also to determine if major friction reducer interactions were caused only by ions in the water, or by other components such as hydrocarbons or residual additives, real produced water and river water samples were procured from Shale Water Research Center for the experiments. Water compositions were confirmed by the use of ICP-OES and are detailed in the table.

Note that some of these waters had significant amounts of suspended solids, which could have been responsible for some of the performance differences shown in the results.

Table 4- Real and Synthetic Produced Water Compositions Used in Experiments. SPW=Synthetic Produced Water, SFW=Synthetic Fresh Water

Ion (mg/L)	SPW 120,000 mg/L	SPW 60,000 mg/L	SPW 30,000 mg/L	SFW 3,000 mg/L	Low-TDS 250 mg/L
Na^+	40,715	20,357	10179	971	32.5
Mg^{2+}	650	325	162.5	50	4.35
Ca^{2+}	4,700	2,350	1175	120	45.4
Sr^{2+}	500	250	125	5	0.35
Ba^{2+}	25	12.5	6.25	2	0.106
Cl^-	73,400	36,700	18350	1835	96.3
SO_4^{2-}	8.58	4.29	2.15	3.32	53
HCO_3^-	17.40	8.70	4.35	41.15	90
TDS	120,000	60,000	30000	3,000	250
pH,	7.1	7.10	7.10	8.00	7.4

3.2 Friction Flowloop

Friction reducers lower the frictional energy dissipation of flowing fluid by lowering the friction factor of the solution. Friction factors for turbulent flow are difficult to measure and calculate as explained in the previous chapter. The Darcy-Weisbach relation shown in Eq. 14 can be used to indirectly measure the friction factor changes. If density, velocity, and system parameters are kept constant, friction factor is proportional to pressure drop. The percent friction reduction can be easily measured by using this relationship to compare pressure drop values of the water to that of the water with friction reducer across a tubing system, Eq. 15.

$$\Delta P = \frac{f*2*\rho*u^2*L}{D} \tag{14}$$

$$\%FR = \frac{f_{solvent}-f_{solution}}{f_{solvent}} = \frac{\Delta P_{solvent}-\Delta P_{solution}}{\Delta P_{solvent}} \tag{15}$$

Other methods such as viscosity correlations have been used in other experiments but

rely on the use of empirical approximations and are not as accurate as the pressure drop measurement[47,34,3].

A comprehensive literature review of the systems used to test friction reducers by measuring pressure drop changes led to the development and construction of the Shale Water Research Center friction flow loop, Fig.10, [60]. Particularly the design shown in Fig. 27 in the appendix was used as the basis of the flow loop design [51].

A 0.435'' ID recirculating friction flow loop was built for friction reducer performance testing. A 7-gallon container feeds fluid to the low-shearing progressive cavity pump that delivers steady non-pulsating flow at 5 gpm through 316 L stainless steel tubing.

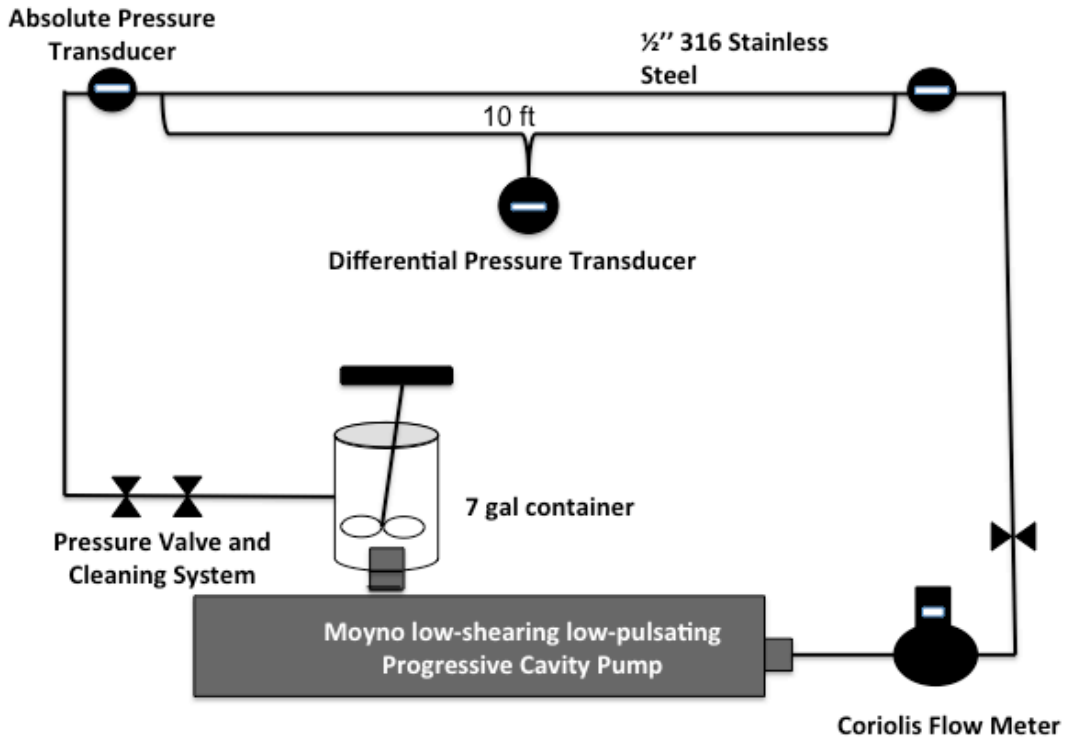

Figure 10-Shale Water Research Center Friction Flow Loop Design

Flow rate, temperature, and density are monitored by a Coriolis flow meter placed 1 ft. downstream of the pump. Pressure drop is measured across a 10 ft. section of straight tubing by two absolute pressure transducers and correlated to friction reduction with Eq. 14 and 15. The distance from the bend to the pressure transducers ensures that the flow is fully developed in the testing section. Pressure drop through the straight tubing section is continuously monitored during the experiments as the fluid recirculates through the loop for approximately 1200 seconds. In the experiment, the friction reducer is directly added to the reservoir tank preloaded with the water to be tested. This is done to simulate "on the fly" addition done in the field.

Experiments were all run at 5 gallons/min resulting in a linear velocity through the testing section of 3.3 m/s with a Reynolds number of 38,000 and shear rate of 2328 s^{-1} for water. The 7-gallon container was filled at all times with 3 gallons of fluid in addition to the system volume of 3.5 gallons. Resistivity measurements confirmed 90% mixing breakthrough after 264 s of having added the solution to the bucket. Experimental results were only considered after the mixing time had passed and the data was smoothed using exponential smoothing.

Figure 11 shows a traditional representation of friction flow loop results. Mixing time is included in the representation , however, the rest of the results shown in this paper will only display friction reduction after the friction reducer has been fully mixed. Inversion from the emulsion into the water was assumed to take place in the 264 seconds of mixing time. As shown by the figure, good field performance is considered to be sustained 50-

80% friction reduction over at least 400-500 seconds.

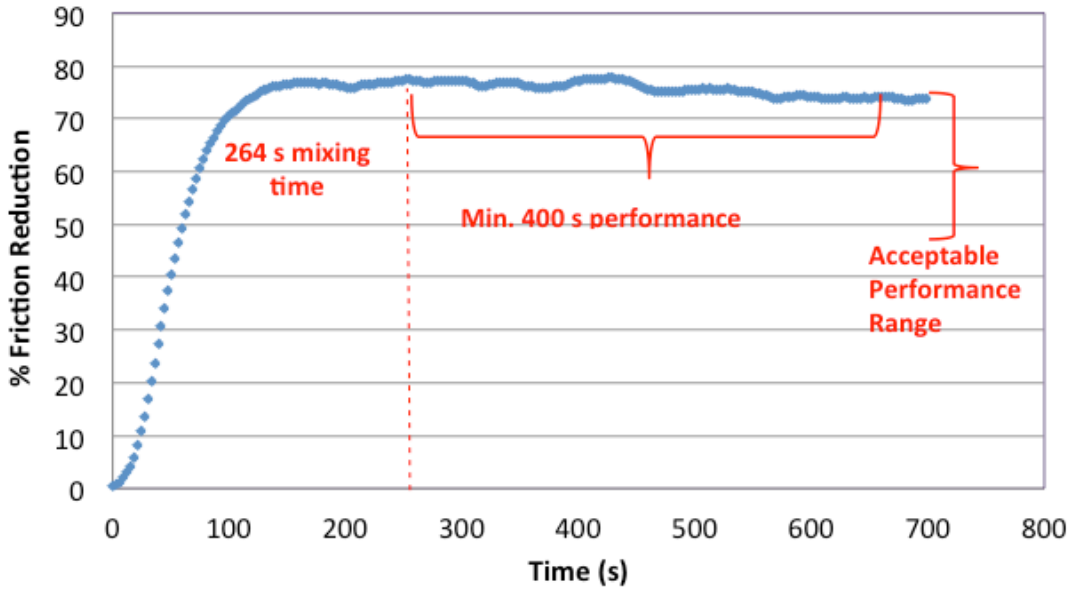

Figure 11-Typical Successful Friction Reducer Performance Curve. 0.5 gpt (150 ppm) of FR-A in low-TDS water.

Chapter 4: Results and Discussion

4.1 Results

4.1.1 Paper Overview

This paper focuses on determining the parameters that affect friction reducer performance by looking at 1) The effect of HPAM degree of hydrolysis (0-30%), 2) the impact of FR concentration, 3) The effect of water quality, and 4) the impact of elevated $Ca^{2+,}$$Mg^{2+,}$ $Fe^{2+/3+}$, and Al^{3+} concentrations in water. The experimental results were used to develop a model to empirically predict friction reducer performance based on the TDS of water,. The model was then validated by comparing the results to friction reducer performance in real produced waters.

4.1.2 HPAM Degree of Hydrolysis

The effect of the polymer degree of hydrolysis on friction reduction was evaluated by measuring the performance of HPAM from 0-30% hydrolysis in 3,000 mg/L synthetic fresh water. Fig. 12 shows the performance increase with increasing degree of hydrolysis. 20% and 30% hydrolyzed polymers maintain their performance between roughly 10% of their maximum performance throughout the 450 seconds while 10% and 0% hydrolysis quickly decrease in performance with similar slopes throughout the studied time interval.

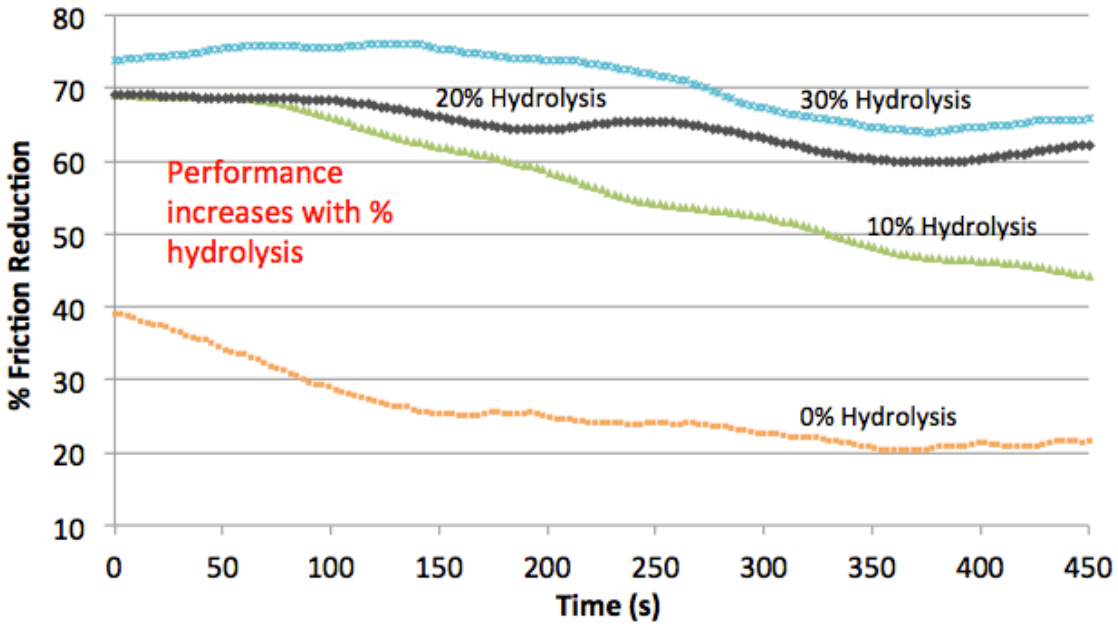

Figure 12- Effect of Polymer Degree of Hydrolysis on Friction Reducer Performance. 1 gpt(300 ppm) of 0-30% HPAM in SFW (3,000 mg/L) over time.

When added to synthetic produced water with a TDS of 120,000 mg/L, the overall friction reducer performance decreases significantly. Fig 13 shows that in the higher TDS brine, the 20% and 10% hydrolysis polymers have a slightly higher performance than the 30% and 0% hydrolyzed polymers. A major difference in the produced water case is that performance in each case is maintained throughout the 500 second observed period while in the synthetic freshwater case performance decreased more than 35% in the 10% hydrolyzed case. Due to the overall low performance in the synthetic produced water case, and because there was only a small difference between 20% and 30% in the produced water case, the 30% hydrolysis polymer was chosen for the rest of the experiments. This was also done because the 30% hydrolysis case is the most commonly used in the industry so it would be more relevant for the rest of the experiments.

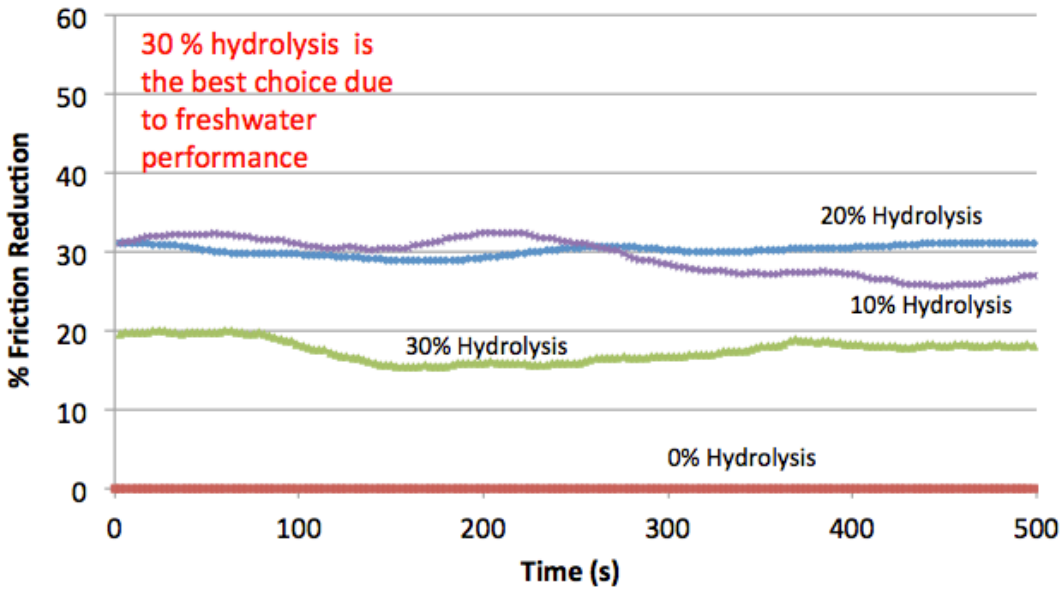

Figure 13-Effect of Polymer Degree of Hydrolysis on Friction Reducer Performance. 1 gpt of 0-30% HPAM in SPW (120,000 mg/L) over time

4.1.3 Concentration Effects on Friction Reducer Performance

The friction reduction abilities of 30% partially hydrolyzed polyacrylamide were tested in low-TDS water at different concentrations to determine the ideal performance concentration. Figure 14 shows the performance of 0.0003 gpt to 2 gpt friction reducer in low TDS water. As shown in the figure, discernable friction reduction can be achieved at concentrations as low as 0.0003 gpt. The results show that at very low concentrations (0.0003 gpt-0.13 gpt) performance increases with increasing concentration, and the performance degradation of the curves are similar. At higher concentrations (0.5 gpt-2 gpt), there is an ideal range at which maximum friction reducer performance is achieved and the increase in concentration seems to decrease overall performance. At 0.25 gpt, the performance degradation is similar to that of lower concentrations, but at higher concentrations performance no longer seems to decrease. Although 0.5 gpt has the

overall highest friction reduction, 1 gpt is a close second and has performance that increases over time so it was chosen as the concentration to use in the rest of the experiments.

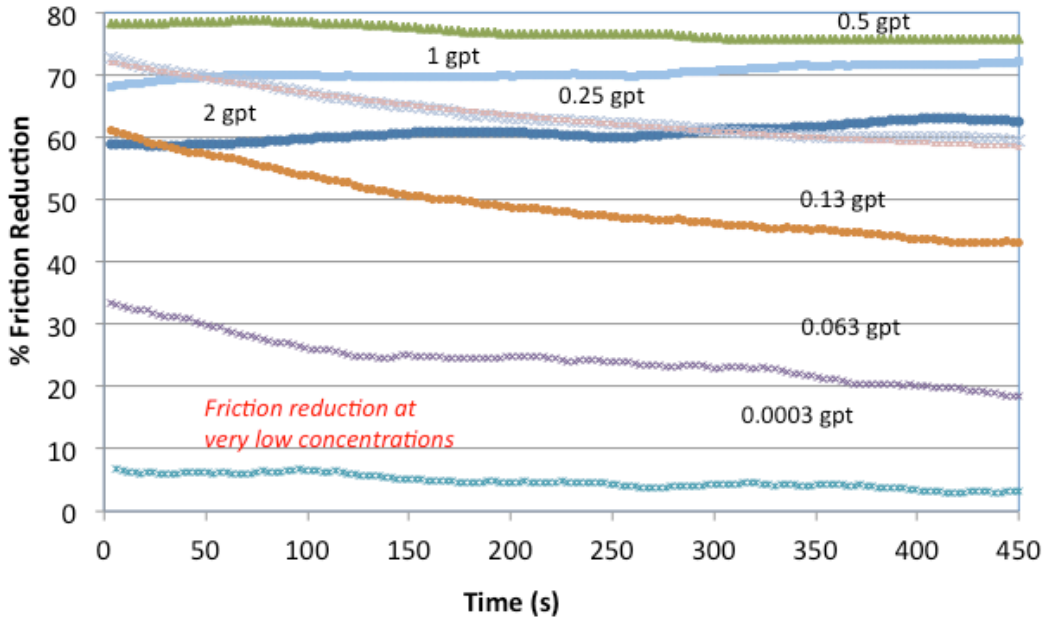

Figure 14- Effects of Polymer Concentration on Friction Reduction. 0.0003 gpt-2 gpt 30% HPAM in Low-TDS Water Over Time. Highest Performance for the 0.5 gpt Case. 0.0003 gpt has Friction Reduction Capabilities.

4.1.4 Effects of Water Quality on Friction Reduction

4.1.4.1 Synthetic Produced Water Effect

The effects of ions on 1 gpt (300 ppm) 30% HPAM was tested in 120,000 mg/L, 60,000 mg/L, and 30,000 mg/L synthetic produced water and in 3,000 mg/L synthetic freshwater (Fig.15). As expected, the overall performance decreased with increasing TDS. However, degradation rates were different for different TDS concentrations. The performance degradation increased with increasing TDS from 3,000 to 60,000 mg/L but stopped

decreasing at 120,000 mg/L where the performance was more or less constant throughout the studied time period.

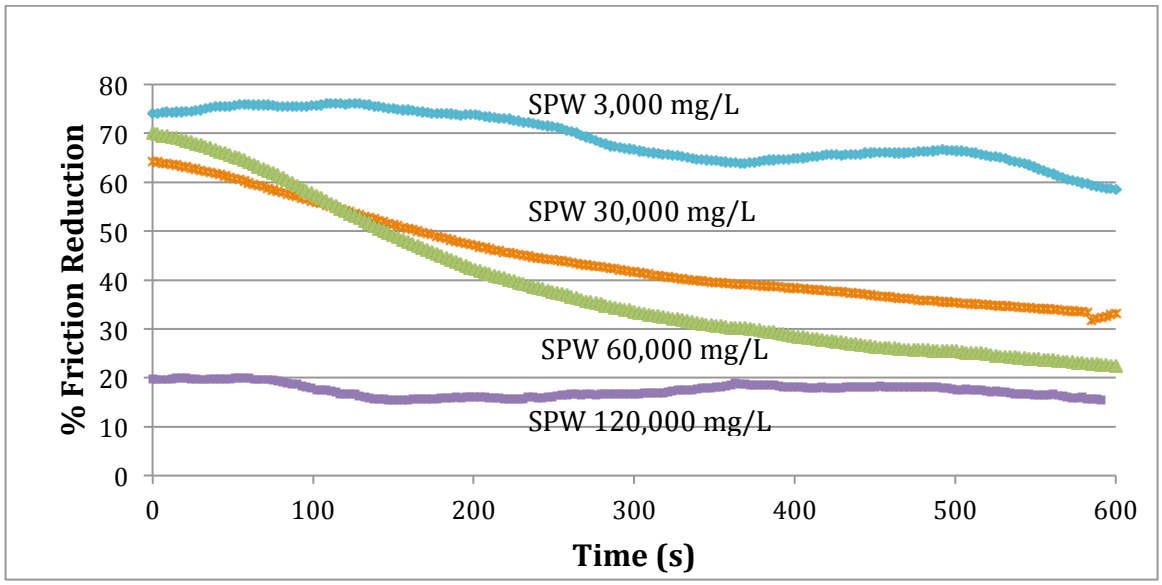

Figure 15- Friction Reduction of 1 gpt(300 ppm) of 30% HPAM in Synthetic Produced Waters from 3,000-120,000 mg/L. Performance decreases with increasing TDS.

When tested in solutions of the same TDS but composed only of NaCl and water, the friction reduction curves were much higher for all of the cases. Even the 120,000-mg/L case shown in Fig. 16, which had 400 s retardation to maximum friction reduction, was able to reach the 70-75% friction reduction range. This shows the importance of multivalent cation concentration on friction reducer performance and the retardation effect that monovalent cations have on friction reduction.

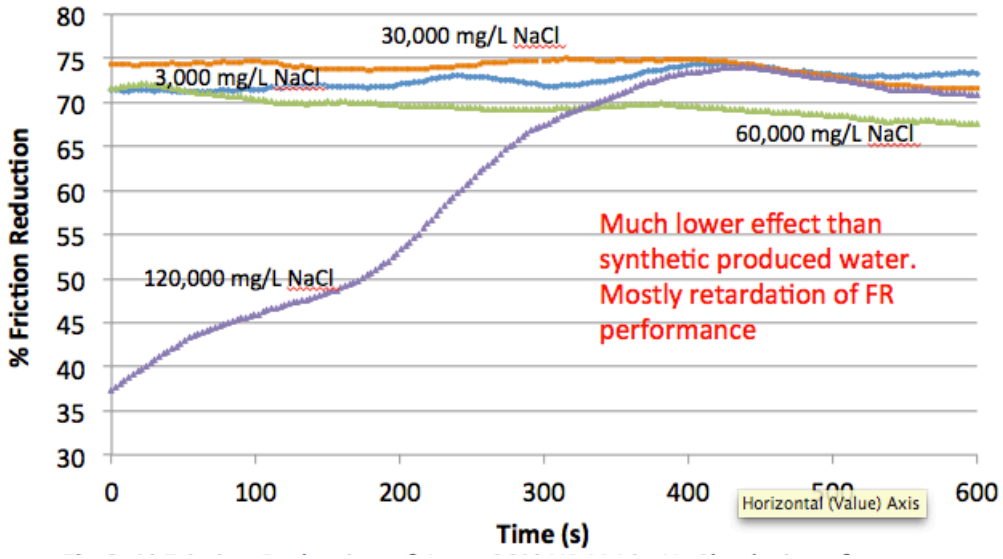

Figure 16- Friction Reduction of 1 gpt (300 ppm) 30% HPAM in NaCl-only Solutions of 3,000-120,000 mg/L. Performance Degradation lower than in the Multivalent Cation Solution.

Ion-valence is not the only factor affecting friction reduction. When looking at 30% HPAM in low-TDS water containing equal molar concentrations of magnesium and calcium, the effect of the calcium ion is much larger than that of the magnesium ion.

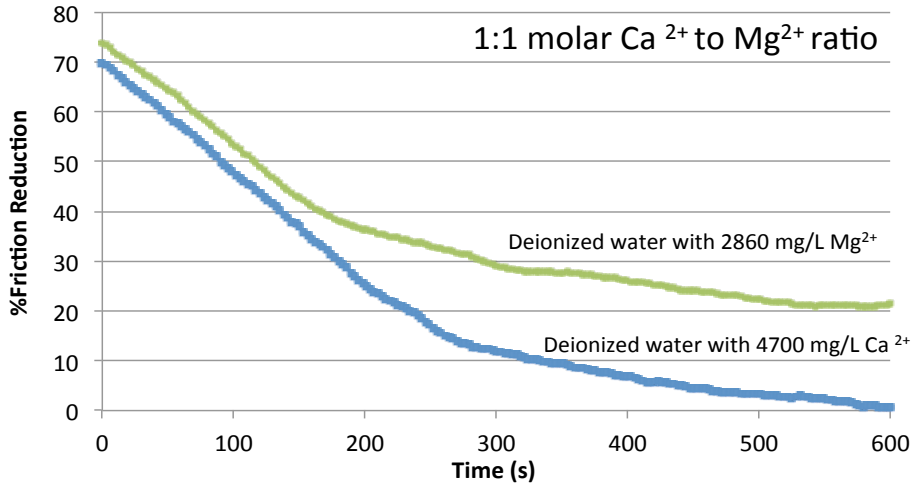

Figure 17 - Friction Reduction of 1 gpt 30% HPAM in low-TDS water with 2,860 mg/L Mg2+ and 4,700 mg/L Ca2+ respectively (1:1 molar ratio). Ca2+ has a higher effect on friction reduction

At these concentrations of 4,700 mg/L Ca and 2860 mg/L Mg, both chloride salts are soluble in water. The ion size, however, is different in each case. Ca^{2+} when hydrated is surrounded by eight water molecules the reported ionic radius is of 1.12 angstroms. Mg^{2+} is hydrated with only six water molecules and its reported ionic radius is of 0.76 angstroms (Persson 2010). Important to note in this experiment is that the calcium solution has a higher initial friction reduction but faster degradation and lower performance than the synthetic produced water solution that has the same calcium concentration and high concentrations of other ions in solution. This shows that calcium and magnesium alone have a higher effect on friction reducer degradation than overall TDS does.

4.1.4.2 Effect of trivalent cations on friction reduction

The effects of aluminum and iron on friction reduction were tested in deionized water to determine the effect that higher ion valence had on friction reduction.

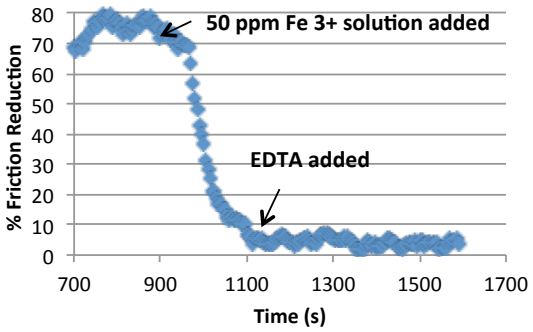

Figure 18a Figure 18a-Friction Reduction of 1 gpt (300 ppm) FR-A in low-TDS water with the addition of 50-ppm Fe(III) solution and EDTA. Friction Reduction Completely Degraded.

Fig 18a shows 1 gpt of FR-A in low-TDS water performing between 70-80%. After 900 seconds, 50 ppm of Fe^{3+} is added as a $FeCl_3$ solution in deionized water. Within 200 seconds of the Fe addition, performance decreases to less than 10%. The addition of EDTA does not revert the effects. The same experiment was performed with 20 ppm of Fe3+.

The lower iron concentration it took over 2000 seconds from the addition to the solution to degrade the performance to a constant value of around 18%, slightly higher

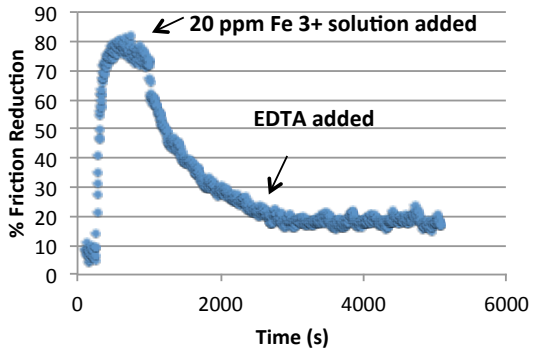

Figure 18b-Friction Reduction of 1 gpt FR-A in low-TDS water with the addition of 20 ppm Fe(III) solution and EDTA.

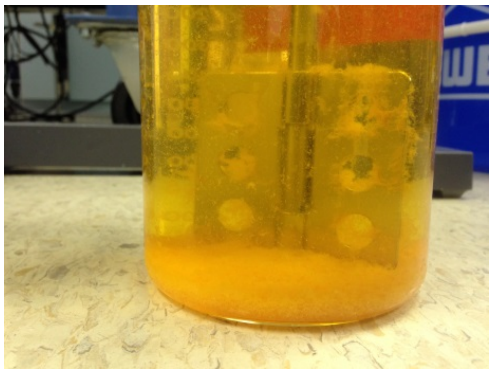

Figure 19-1 gpt of FR-A in low-TDS water with 50 ppm Fe (III) in a Beaker

than the 50 ppm case. Fig 19 shows a picture of the flocculation that occurs when 50 ppm of iron (III) is added to a 1-gpt solution of FR-A. The gel precipitates in the beaker formed immediately after the addition of the iron and attached to the stainless steel paddle and settled to the bottom of the beaker.

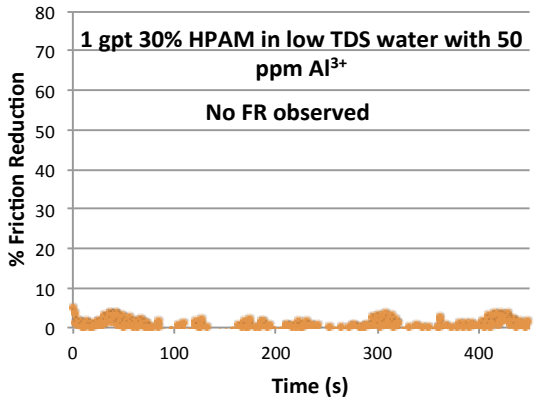

l

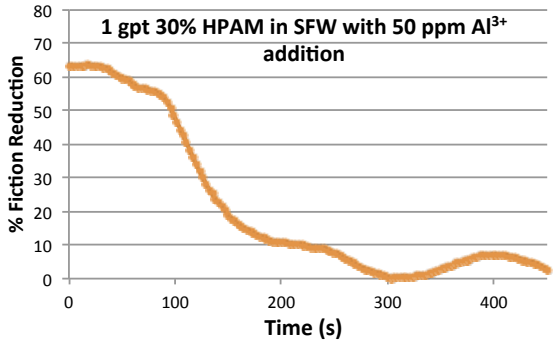

Figure 20a-1 gpt of 30% HPAM in low-TDS water with 50 ppm Al(III). No friction reduction.

Figure 20b-1 gpt of 30% HPAM in low TDS-water. Addition of 50 ppm Al(III) lowers friction reduction.

The consistency was that of a gel and the flocs were orange colored. ICP results of the water solution showed that only 72% of the Fe originally added to the water remained in solution confirming that Fe was in the gel phase.

Aluminum showed similar performance as the iron solution did. Fig 20a shows that there was no measurable friction reduction in a solution of 1 gpt 30% HPAM in low TDS water with 50 ppm Al^{3+}. Fig 20 b shows the performance degradation to below 10% in 200 seconds after the addition of 50 ppm Al^{3+} as $AlCl_3$. Precipitation was also observed in the beaker experiments but there were less precipitates settled at the bottom of the beaker than in the iron experiments, and the floc color was white due to the aluminum (Fig.21).

Figure 21-1 gpt 30 % HPAM in low-TDS water with 50 ppm Al(III) in a Beaker

4.2 Discussion

4.2.1 Discussion on Experimental Results

The experimental results show the importance of knowing the effects of friction reducer characteristics, and the interactions with ions in water. A higher degree of hydrolysis, or higher percentage of negative charges, creates a higher electrostatic repulsion and encourages polymer stretching. However, the higher degree of negative charges also leads to higher ion-polymer interactions that effectively reduce the size of the polymer chain and can permanently degrade the friction reducer. Fig. 12 shows the increasing friction reducer performance with increasing degree of hydrolysis in a moderate brine of 3,000 mg/L. All polymers seem to be affected relatively the same by shear degradation

and ionic interaction. At these low water concentrations, a higher degree of hydrolysis such as 30-40% should be the polymer of choice (avoid going too high as interactions with metals in the formation could make polymer clean-up extremely difficult). The experiments of degree of hydrolysis in synthetic produced water show the degradation effect of metal ion concentration on friction reduction. In this case the ions in solution lower the overall radius of gyration of the polymers making them less susceptible to shear degradation and chain scissoring. Although a lower overall value, the performance is kept relatively constant throughout the run. The 30% hydrolysis performed best in the SFW experiments and the 10% and 20% hydrolysis polymers performed slightly better than the 30% in the produced water experiments. The difference in performance is insignificant in produced water but significant in freshwater, so the 30% polymer was chosen for the rest of the experiments.

Polymer-polymer interactions are also important. The critical overlap concentration, the concentration at which the solution goes from the dilute to the semi-dilute regime, is affected by polymer length, type and solution quality. Knowing the critical overlap concentration value for the friction reducer being used in the field is important to ensure

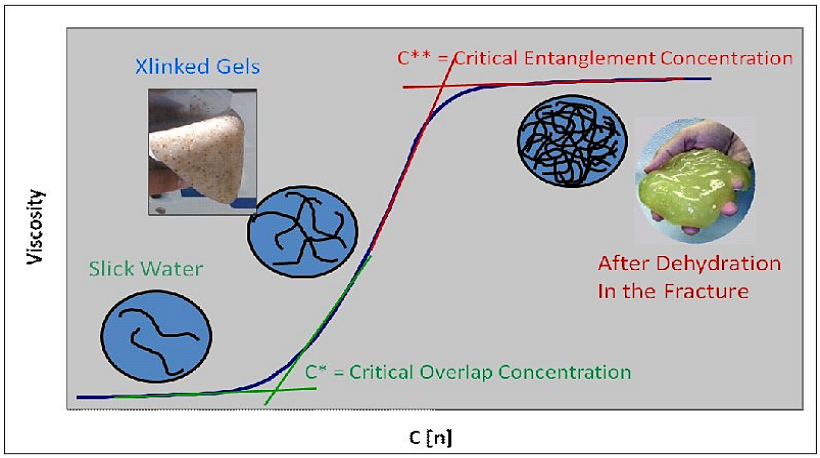

Figure 22-Viscosity of a Solution as a Function of Polymer Concentration [40]

maximum performance at the lowest chemical dosage possible, and to avoid excessive floc formation. Using Eq. 13, the critical overlap concentration is around 1976 ppm of friction reducer, however, experimental results show that antagonistic interactions begin much before that. Fig. 14 shows that for the 10,000,000 Da 30% HPAM, the ideal performance range is around 0.5-1 gpt (150-300 ppm active polymer). At concentrations higher than this (2 gpt) polymer-polymer interactions begin to interfere with the stretching of the polymer, decrease friction reducer performance, and increase floc/gel formation. Concentrations above the critical overlap concentration into the semi-dilute region are used for cross-linked gel formation. At high ion concentrations, and too high friction reducer concentrations, cross-linked gel might form either homogeneously or heterogeneously throughout the solution. Dosing in industry wells is usually determined by using concentrations used in previous wells in the region, and often when the desired pressures are not reached after polymer dosing, more friction reducer is added to the well. Overdosing could be detrimental to the operation, particularly if the initial friction reducer concentration that was added is close to the critical overlap concentration. It is essential to know the chemical make-up of the friction reducer used, or to perform flow loop experiments to understand the polymer behavior and prevent polymer overdosing.

Water quality, as shown by Fig. 15-17, has the biggest effect on friction reducer performance. The produced water experiments, and individual NaCl and $Ca^{2+/}Mg^{2+}$ experiments show the effect that different cations have on friction reducers. Extremely high concentrations of monovalent cations (120,000 mg/L NaCl) have a retardation effect on friction reduction, but do not lower the performance to the levels that lower

concentrations of brines with multivalent cations do (30,000 mg/L). The polymer-ion interactions are different for both cases. Increased Na^+ concentration has a shielding effect on the polymer. Monovalent cations shield the negative charge on the polymer, reducing the free energy of the coiled state, and causing it to coil more. Shear rate, however, can still mechanically stretch the polymer, increasing friction reduction until the maximum performance is attained. The 120,000-mg/L line in fig 16 shows the shielding effect and the subsequent shear stretching effect on the polymer.

Fig. 17 shows the effect that divalent cations have on polyacrylamide. In this experiment a maximum friction reduction of 70-80% is attained but slowly decreases to 0 and 20% for the Ca^{2+} in deionized water and Mg^{2+} in deionized water case respectively. This suggests that the divalent cations affect the polymer differently than monovalent cations do. The discrepancy between magnesium and calcium values shows the importance of the ion size on friction reduction. The higher valence on the divalent cations not only shields the polymer charge, lowering the free energy of the coiled state, but also has the ability to inter and intra molecularly bridge two sections of polymer together. This dramatically reduces polymer linearity, and in some cases, forms branches that could cause an increase in turbulence. Larger (hydrated)

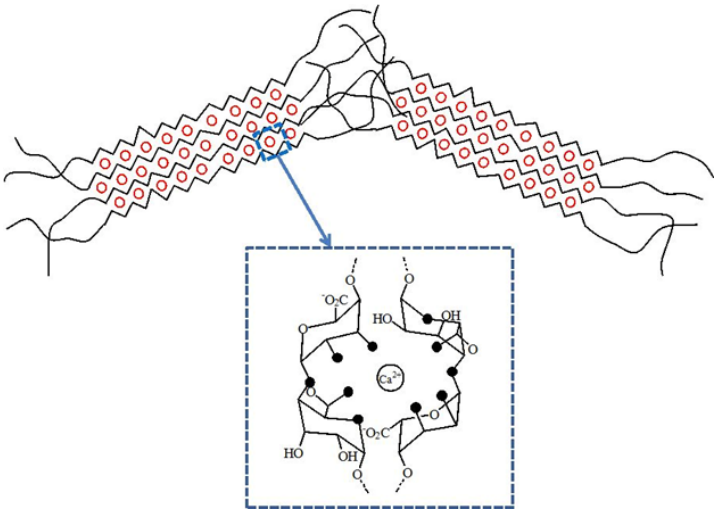

Figure 23- Calcium and Polymer Bridging

ions can bridge more polymer segments and have a larger effect as seen by the calcium and magnesium experiments.

Ion-ion interactions play a crucial role on the effect of produced water on friction reduction. Comparing the friction reducer performances in Fig. 24 of the 120,000-mg/L NaCl solution to that of 120,000 mg/L SPW with 4,700 mg/L Ca^{2+} to that of a solution containing only 4,700 mg/L of Ca^{2+} the effect that ion interactions have on performance can be seen. The synthetic produced water case starts at the lowest friction reduction but experiences the least amount of change in performance from all the cases. While the NaCl solution increases with time due to the shear rate effect, the Ca^{2+}-only solution decreases due polymer bridging, and the synthetic produced water solution stays constant. The presence of various types of multivalent cations is what causes the synthetic produced water to have such a low average friction reduction, but also to have a lower degradation than the calcium alone case. The high concentration of monovalent cations in the SPW shields the negative charges on the polymer making it less susceptible to polymer bridging from multivalent cations. This effect "protects" the friction reducer from degrading to levels as low as those from having calcium concentration alone. When

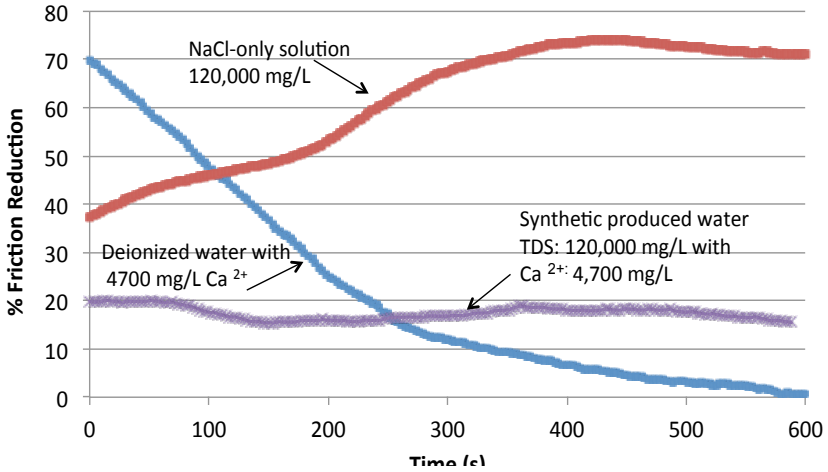

Figure 24- Effect of ion-ion interactions on friction reducer performance.1 gpt 30% HPAM in different water qualities

there is high divalent cation concentration, the addition of monovalent cations can actually improve polymer performance and reduce degradation.

4.2.2 Trivalent Cation Effect: Iron and Aluminum

The rapid friction reducer degradation and flocculation at low concentrations of iron and aluminum is a major problem for the oil and gas industry. The precipitate that forms sticks in the formation and is difficult to clean and break-up. This causes huge costs for the industry and can cause formation damage that leads to reduced well production. Several studies have focused on the flocculation of polyacrylamide with metals, particularly because HPAM was first used in the water treatment industry to flocculate heavy metals out of the water. The main difference between the behavior of aluminum and iron compared to that of the divalent and monovalent cations is their low solubility and speciation in water. Iron and aluminum are mostly in hydroxide form in solution or as precipitated small particles on which the friction reducer can adsorb to.

NMR, light scattering, and modeling experiments have shown that for aluminum, the most significant interactions are those of Al^{3+} (at pH<4) and $Al_{13}OH_{36}{}^{3+}$ at higher pH values. The relevant interactions are of COO---Al and COO_3-----Al_{13} type. At high polymer concentrations (above the critical overlap concentration) aluminum could be used as a cross linker and form a uniform polymer-aluminum gel. At lower polymer concentrations, or in the presence of electrostatic shielding by other ions, the observed precipitation in Fig.21 forms (Rahbari, Sarazin and Francois 1989).

Larger insoluble $Al(OH)_3$ particles can even hydrogen bond with the amide group of the polymer and increase precipitation. HPAM adsorption experiments onto alumina covered silica particles, showed that the amide group adsorbs onto the particle through hydrogen

bonding with the "free hydroxides" on the surface (Pefferkorn, et al. 1990). Similar results were shown with hematite and quartz experiments. Published IR spectra results show that there was a change in the NH_2 and COO^- group bands of HPAM with the addition of ferric iron suggesting that a bond had been formed (Jin, Hu and Hou 1987). Adding NaCl can reduce the hydrogen bonding, but hematite and alumina is still highly flocculated. This flocculation is the major effect that these trivalent cations have on friction reduction. Although the soluble "Free" Al^{3+} and Fe^{3+} ions have a bridging effect similar to that of calcium, the major effect is the flocculation that occurs due to adsorption onto the solid precipitates. Knowing the water quality, and removing these solids from the water solution is an important water treatment method to prevent friction reducer degradation.

4.2.3 Model to Predict Friction Reduction based on Water Quality

An empirical equation was developed to predict friction reducer performance as a function of water TDS. The data collected for 1 gpt 10,000,000 Da, 30% HPAM in the varying synthetic produced waters was used to fit a correlation between friction reduction and water quality. Due to the complexity of the ion-polymer and ion-ion effects on friction reduction, and the difficulty to quantify them, an empirical approach was needed to easily and quickly estimate the polymer performance in different waters at different times.

The exponential decay model used is of the form

$$\%FR = y_0 + a\exp(-kt) \quad (16)$$

where y_o represents the friction reduction at long times, a is the change between the initial friction reduction and the final value, and k is a decay constant.

The fitted parameters as a function of TDS are

$$y_o = 15.07 + 30.766\exp(-0.0239[\text{TDS}]) \quad (17)$$

$$a = -0.00026[TDS]^3 + 0.0368[TDS]^2 - 1.0371[TDS] + 40.497 \quad (18)$$

$$k = 0.0004 + 0.0046 * \exp(0.055[TDS]) \quad (19)$$

Figure 25 shows the model (red line) compared to the data that was used to fit it (shown in Fig. 15). The figure highlights the noisiness of the original data, but that the model used predicts the trend well for low and high produced water concentrations.

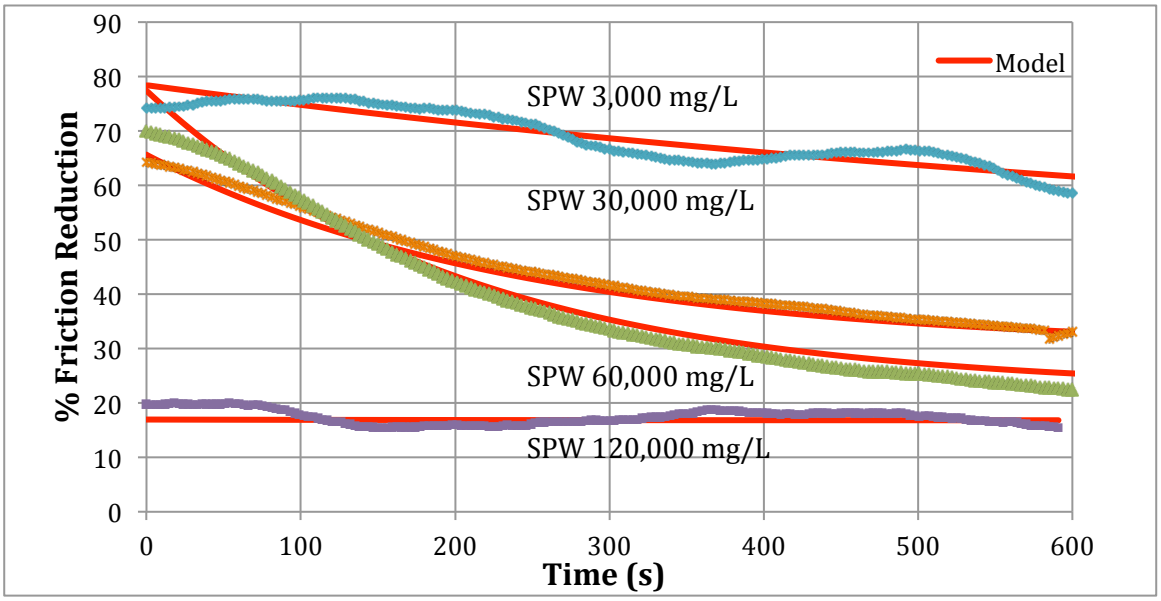

Figure 25- Fitted Exponential Decay Model to 1 gpt (300 ppm) 30% HPAM in SPW from 3,000 mg/L to 120,000 mg/L

The first 100 seconds have the largest deviation from experimental data as can be seen by the residual plot in Fig, 26 ($\%FR_{measured}$ -$\%FR_{model}$). In this first time block, the model overestimates the initial friction reduction for the 3,000 mg/L, 30,000 mg/L and 60,000 mg/L by up to 4%, 1.4%, and 7.5% respectively. It slightly underestimates the 120,000 mg/L case by 2.8%. During the rest of the experiment, Fig. 26 shows that the model predicts the observed data within 2.3%. Fig. 25 also shows that the model is able to predict the slow friction reducer degradation at high and low concentrations, and the rapid degradation at intermediate concentrations.

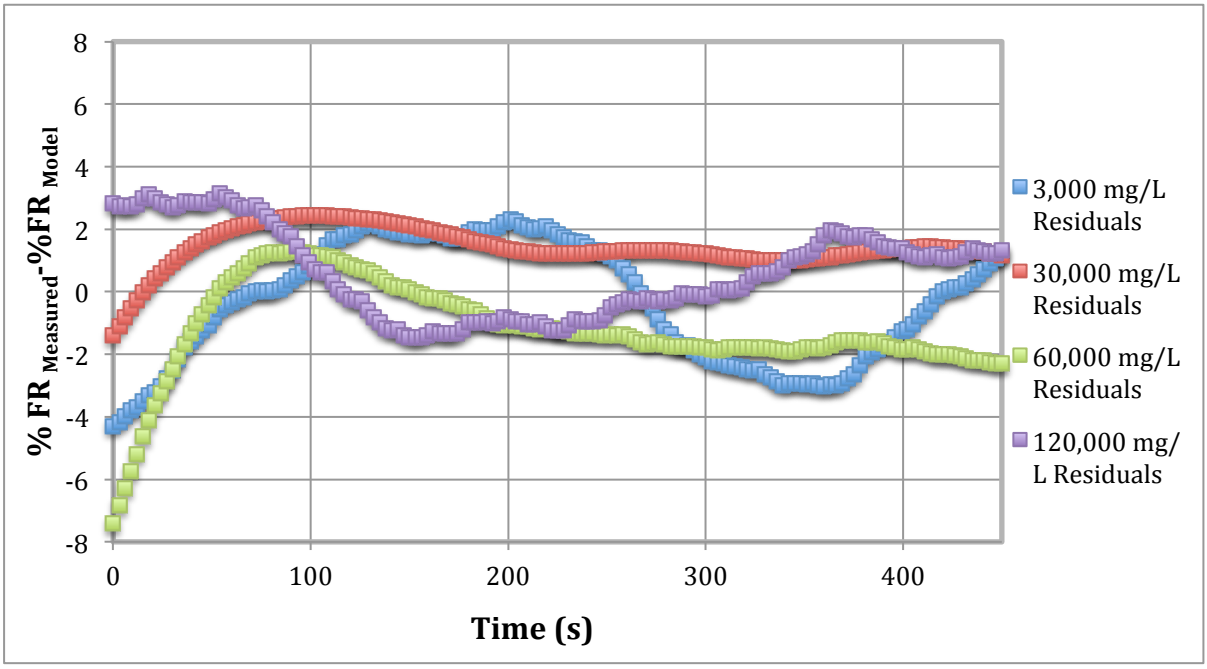

Figure 26 – Plot of Residual Values (%FR measured-% FR predicted) between model and experimental data from Fig. 25 as a function of time

Note that this equation is meant to be used at time intervals of similar magnitude to the 400 seconds studied in these experiments, and does not accurately represent the effects of

shear rate at very long intervals. The major limitation of the model is that it is purely empirical and based on experimental results from one type of polymer and not on any mechanisms. As such, it fails to predict performance in waters that are not of similar relative ion concentrations as the synthetic produced water used and of polymers that do not behave like the 10,000,000 Da 30% HPAM that was used. It also does not account for the effects of other fracturing additives, the impact of oxidative agents, or concentration effects. However as shown in the figures, it works well for HPAM, and waters of similar composition used for the ones in this experiment.

The applicability of the model was tested on a generic HPAM-based friction reducer in produced waters of varying TDS concentration. The result is shown in Fig 27. The model still has good agreement with the real data even though the water and polymer compositions are not the same as the ones used to fit the model.

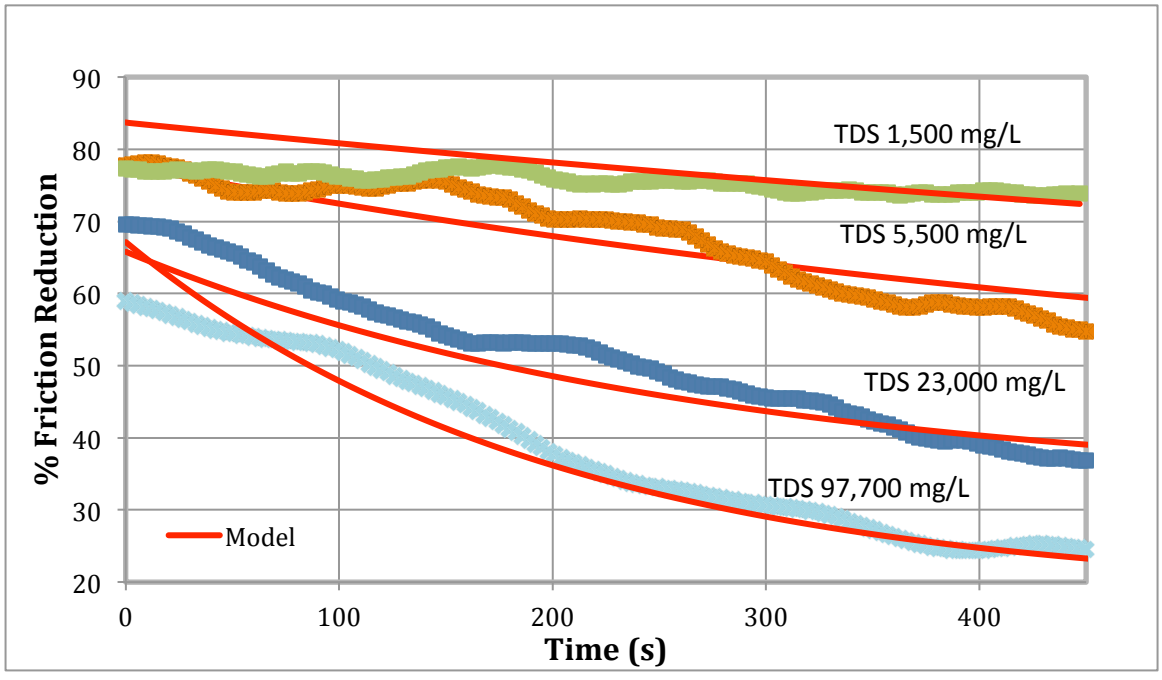

Figure 27- Fitted Exponential Decay Model to 1 gpt (300 ppm) FR-A in Real Produced Water from 1,500 mg/L to 97,700 mg/L

Figure 27 and the residual graph of Fig. 28 show that the model (just as in Fig.25) deviates the most from the observed data in the first 100 seconds. In this real produced

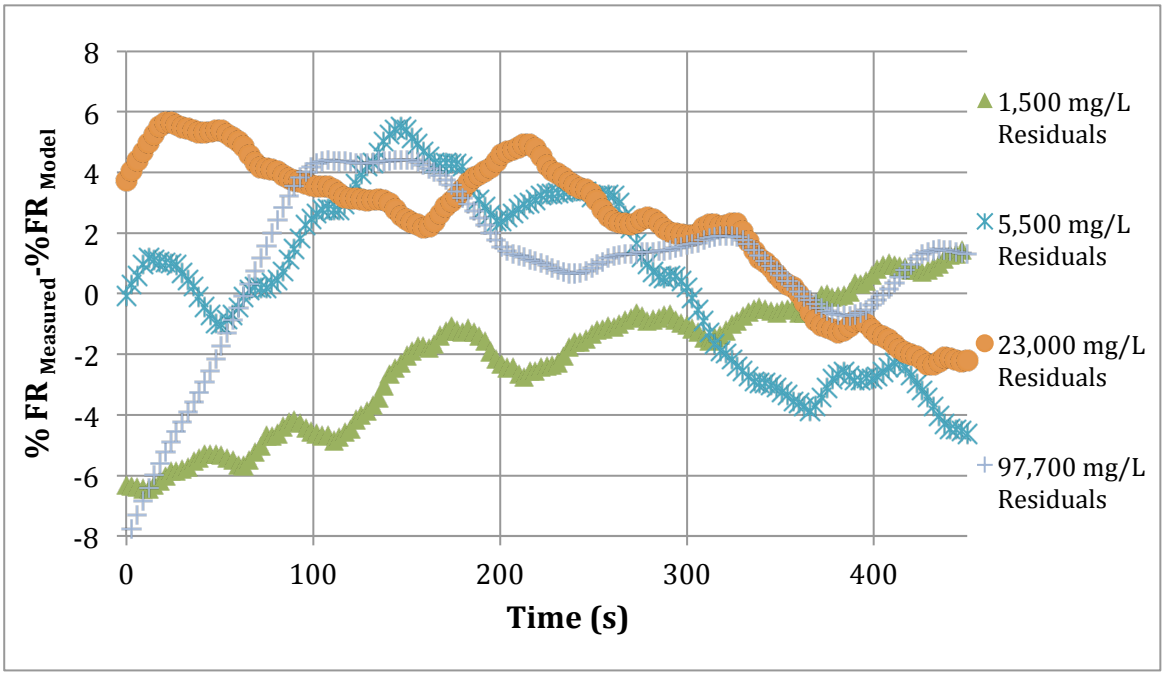

Figure 28 - Plot of Residual Values (%FR measured-% FR predicted) between model and experimental data from Fig. 28 as a function of time

water experiment the model overestimates the friction reduction for 1,500 mg/L and 97,700 mg/L by up to 6.9% and 7.8% respectively. It slightly underestimates the values for the 5,500 mg/L by 1.5% in the first 100 seconds and 5.3 % in the first 200 seconds. The 23,000-mg/L curve is overestimated by up to 5.3% over the experimental period. As can be seen by comparing Fig. 28 to Fig. 26, the quality of the is fit is much lower overall than for Fig. 25, but still predicts the data well. The maximum deviation from the measured data is 7.75% in the first 100 seconds. After the first 100 seconds, the model remains within 5.3% of the observed data, despite the fact that real friction reducer and

produced water was used. Table 3 shows the difference between the calculated and observed friction reducer degradation (%FR initial-% FR final). As expected, the values that correspond to the synthetic produced water and 30% HPAM have better agreement with the data than the real FR and produced water case. Nonetheless, the largest deviation is of 8.83% for the real produced water case. A good fit for quick field estimation.

Table 3-Calculated and Measured Friction Reduction Degradation over Experimental Period in Synthetic and Real Produced Waters

1 gpt 30% HPAM in Synthetic Produced Waters				
$\%FR_{initial}$-$\%FR_{final}$	3,000 mg/L	30,000 mg/L	60,000 mg/L	120,000 mg/L
Calculated	18.22	32.52	51.94	0.02
Measured	15.57	31.15	47.56	4.29
Difference	2.64	1.37	4.38	-4.27
1 gpt FR-A in Real Produced Waters				
$\%FR_{initial}$-$\%FR_{final}$	1,500 mg/L	5,500 mg/L	23,000 mg/L	97,700 mg/L
Calculated	11.36	18.41	26.74	44.53
Measured	3.49	22.90	32.67	35.70
Difference	7.87	-4.49	-5.93	8.83

The fit of the model is difficult to quantitatively describe using conventional statistical tools due to the raw data being “noisy” and thus any resulting values do not accurately describe the predictive abilities of the model. A more mechanistic approach is needed to theoretically and statistically validate the quality of the model. However, by observation of the fit in figure 25-29, the model provides a good estimate of friction reducer behavior in waters of different TDS.

Chapter 5: Conclusion and Future Work

5.1 Conclusion

In summary, a characterization of typical friction reducer behavior in field conditions was shown in the paper, and an empirical equation to predict performance was proposed. The importance of polymer hydrolysis and concentration was explained, and 1 gpt (300 ppm) 30% HPAM showed the best performance among the studied polymers. Experiments performed on friction reducer degradation in synthetic produced waters of varying qualities 3,000-120,000 mg/L, showed that increasing produced water TDS decreased friction reducer performance. More detailed experiments on friction reducer performance in NaCl-only solutions showed that the monovalent cations have a retardation effect on FR performance at very high concentrations (120,000 mg/L), but do not degrade the polymer performance in the time intervals of interest. The charge shielding effect by the monovalent cations reduces the multivalent cation degradation effect by shielding the polymer. NaCl can be used in produced waters with high multivalent cation concentration to lower performance degradation. Low concentrations of insoluble trivalent cations such as Al^{3+} and Fe^{3+} can lower the polymer performance down to 0% friction reduction and precipitate gels out of solution that can cause formation damage.

Finally, an empirical model was proposed to easily estimate HPAM friction reducer performance in produced water and was shown to provide good predictions for FR performance in real and synthetic produced waters.

5.2 Future Work

Future work needs to focus on a deeper understanding of the $Fe^{3+,}$ and Al^{3+} flocculation and how to revert it. Currently when gel precipitates occur in the field, operations need to be shut down and expensive acid treatments are done to try to remove them from the formation. Finding a way to reduce the polymer attachment onto the Fe and Al surfaces would be of great benefit to the industry.

Advances in fluid mechanics and polymer research will allow for the development of a more mechanistic approach and equation to predict friction reducer performance.

Exploration of non-acrylamide based polymers is the primary area where future research should be headed. HPAMs were originally used in water treatment to flocculate heavy metals out of solution, and as such interact very strongly with any ion in solution. Finding an alternative polymer that is not as electrostatically vulnerable to the ions in solution would prevent most of the problems with friction reducers in the industry.

Nomenclature and Symbols

Re- Reynolds Number

u-Velocity

$\mathbf{L_c}$-Characteristic Length

ν-Kinematic (Fink 2013) (Economides 2007)Viscosity

μ-DynamicViscosity

ρ-Density

$\mathbf{L_h}$-Hydrodynamic Entrance Length

D-Pipe Diameter

γ-Shear Strain

τ- Stress

$\mathbf{f_D}$-Friction Factor Darcy

$\mathbf{f_f}$-Fanning Friction Factor

ε-Surface Roughness

K- Consistency Index

n- Power Law Exponent

χ-Flory-Huggins Interaction Parameter

$\mathbf{l_B}$-Bjerrum Length

κ-Debye Length

z-Ion Charge

ΔP-Pressure drop

SWRC-Shale Water Research Center

SPW-Synthetic Produced Water

SFW-Synthetic Fresh Water

FR- Friction Reducer

GPT-Gallon per Thousand Gallons

References

1. Abd-El-Aziz, Alaa S. *Macromolecules Containing Metal and Metal-Like Elements, Organoiron Polymers (Volume 2).* Wiley-Interscience, 2003.
2. Abubakar, A., et al. "Parameters of Drag Reducing Polymers and Drag Reduction Performance in Single-Phase Water Flow ." *Advances in Mechanical Engineering*, 2014.
3. Adachi, Yasuhisa. "Polyelectrolyte Dynamics ." In *Encyclopedia of Colloid and Interface Science* , by Tharwat Tadros, 931-944. Springer Berlin Heidelberg, 2013.
4. Aften, C.W., W.P. Watson, and Kemira Chemicals. "Improved Friction Reducer for Hydraulic Fracturing." *SPE Hydraulic Fracturing Technology Conference* . The Woodlands: SPE, 2009. SPE 118747.
5. Aften, Carl. "Study of Friction Reducers for Recycled Stimulation Fluids in Environmentally Sensitive Regions." *Society of Petroleum Engineers*, 2010: 138984.
6. Bazant. "MITOpenCourseware." *Electrostatic Correlations* . 2011. http://ocw.mit.edu/courses/chemical-engineering/10-626-electrochemical-energy-systems-spring-2011/lecture-notes/MIT10_626S11_lec28.pdf (accessed 12 19, 2014).
7. Bergman, Theodore, Adrienne Lavine, Frank Incropera, and David Dewitt. In *Fundamentals of Heat and Mass Transfer*, by Theodore Bergman, Adrienne Lavine, Frank Incropera and David Dewitt, 389-391. Jefferson City: John Wiley & Sons, 2011.
8. Bird, Byron, Warren Stewart, and Edwin Lightfoot. *Transport Phenomena.* New York: John Wiley & Sons , 2006.
9. Brostow, Witold. "Drag Reduction in Flow: Review of Applications, Mechanism, and Prediction ." *Journal of Industrial Engineering Chemistry* , 2008: 409-416.
10. Carman P.S.l Cawiezel, K.E. "Succesful Breaker Optimization for Polyacrylamide Friction Reducers Used in Slickwater Fracturing ." *SPE* , 2007: 106162.
11. Carman, P.S., and Cawiezel K.E. "Successful Breaker Optimization for Polyacrylamide Friction Reducers Used in Slickwater Fracking." *SPE Hydraulic Fracturing Technology Conference* . College Station: SPE, 2007. 106162.
12. Caruso, Mary, et al. "Mechanically-Induced Chemical Changes in Polymeric Materials." *Chemical Reviews* , 2009.
13. Cengel, Yunus, and John F Cimbala. *Fluid Mechanics: Fundamentals and Applications* . McGraw-Hill , 2010.
14. Chanda, Manas. *Advanced Polymer Chemistry* . CRC, 2000.
15. —. *Advanced Polymer Chemistry: A Problem Solving Guide.* New York: Marcel Dekker, 2000.
16. Cowan, Martin, Chad Garner, Roger Hester, and Charles McCormick. "Water-Soluble Polymers. LXXXIII. Correlation of Experimentally Determined Drag

Reduction Efficiency and Extensional Viscosity of High Molecular Weight Polymers in Dilute Aqueous Solution." *Journal of Applied Polymer Science*, 2000: 1222-1231.
17. Economides, Michael. *Modern Fracturing: Enhancing Natural Gas Production* . Energy Tribune Publishing Inc, 2007.
18. Farinato, Raymond, and Paul Dubin. *Colloid-Polymer Interactions: From Fundamentals to Practice.* Wiley-Interscience, 1999.
19. Ferguson, Marcelle, and Michael Johnson. "Comparing Friction Reducers' Perfornance in Produced Water from Tight Gas Shales." *Journal of Petroleum Technology* , 2009: 24-27.
20. Fink, Johannes. *Hydraulic Fracturing Chemicals and Fluids Technology* . Gulf Professional Publishing, 2013.
21. Fitzpatrick, Richard. "No Slip Condition." *University of Texas.* April 27, 2012. http://farside.ph.utexas.edu/teaching/336L/Fluidhtml/node84.html (accessed December 29, 2014).
22. Gadd, G.E. "Reduction of Turbulent Fraction by Dissolved Additives." (Nature) 1966: 224-253.
23. Goddard, E.D. *Interactions of Surfactants with Polymers.* CRC Press, 1992.
24. Goudar, Chetan, and Jagadesh Sonnad. "Explicit Friction Factor Correlation for Turbulent Flow in Smooth Pipes." *Industrial & Engineering Chemistry Research* , 2003: 2878-2880.
25. Hawkins, W.L. *Polymer Degradation and Stabilization.* Springer, 2011.
26. Hershey, Harry, and Jacques Zakin. "A Molecular Approach to Predicting the Onset of Drag Reduction in the Turbulent Flow of Dilute Polymer Solutions ." *Chemical Engineering Science*, 1967: 1847-1857.
27. Hoyt, J.W. "Effect of Ferric Ions on Drag Reduction Effectiveness of Polyacrylamide." *Polymer Engineering and Science* , 1980: 493-498.
28. Hoyt, J.W., and A.G. Fabula. "The Effect of Additives on Fluid Friction." *Naval Hydrodynamics*, 1964.
29. Hoyt, J.W., and Robert Wade. "Turbulent Friction Reduction by Polymer Solutions." In *Water-Soluble Polymers*, by N.M. Bikales, 137-149. New Jersey: Plenum Press, 1973.
30. Hunston, D.L, and J.L Zakin. "Effects of Flow-Assisted Degradation on the Drag Reduction Phenomenon." *Polymer Preprints*, 1978: 430-438.
31. Jin, Ruiren, Weibai Hu, and Xianjun Hou. "Mechanism of Selective Flocculation of Hematite from Quartz with Hydrolyzed Polyacrylamide ." *Colloids and Surfaces*, 1987: 317-331.
32. Kaufman, P., G.S. Penny, and J. Paktinat. "Critical Evaluations of Additives Used in Shale Slickwater Fracs ." *SPE*, 2008: 119900.
33. Kim, O.K., R.C Little, and R.Y Ting. "The Correlation of Drag-Reduction Effects with Polymer Intrinsic Viscosity." *Journal of Colloid and Interface Science*, 1974: 530-535.
34. Kim, Oh-Kil, and Ling-Siu Choi. "Drag Reducing Polymers ." In *Polymeric Materials Encyclopedia*, by Joseph C Salamone, 1937-1944. Boca Raton : CRC Press , 1996.

35. Loh, Jun Xian. *Polymeric and Self Assembled Hydrogels: From Fundamental Understanding to Applications (Monographs in Supramolecular Chemistry)* . Royal Society of Chemistry, 2012.
36. Lumley, J.L. "Drag Reduction by Additives." *Annual Review of Fluid Mechanics*, 1969: 367-384.
37. McAllister, E.W. "Drag-Reducing Agents." In *Pipeline Rules of Thumb Handbook: A Manual of Quick Accurate Solutions to Everyday Pipeline Engineering Problems*, by E.W. McAllister, 443. Oxford: Elsevier, 2009.
38. Merril, E.W., K.A Smith, and H., Mickley H.S. Shin. "Study of Turbulent Flows of Dilute Polymer Solutions in a Couette Viscometer." *Transactions of the Society of Rheology*, 1966: 335-351.
39. Montgomery, C. "Intrinsic Viscosity of a Solution as a Function of the Polymer Concentration. ." *Fracturing Fluid Components*, 2013.
40. Neff, Jerry, Keneth Lee, and Elisabeth DeBlois. "Produced Water: Overview of Composition, Fates, and Effects." In *Produced Water: Environmental Risks and Advances in Mitigation Technologies*, by Jerry Neff, Keneth Lee and DeBlois Elisabeth, 3-54. New York: Springer, 2011.
41. Paktinat, Javad, Bill O'Neil, Carl Aften, and Hurd Micheal. "The Shearing Effect on Hydrophobically Associative Water-Soluble Polymer and Partially Hydrolyzed Polyacrylamide Passing Through Wellbore Simulation Device `." *Society of Petroleum Engineers*, 2011: 144210.
42. Paktinat, Javad, Bill O'Neil, Carl Aften, and Micheal Hurd. "High Brine Tolerant Polymer Improves Performance of Slickwater Frac in Shale Reservoirs." *Society of Petroleum Engineers*, 2011: 144210.
43. Pefferkorn, A.C, A.C Jean-Chronberg, Chauveteau. G., and Varoqui. R. "Adsorption of Hydrolyzed Polyacrylamided onto Amphoteric Surfaces ." *Journal of Colloid and Interface Science*, 1990: 66-74.
44. Persson, Ingmar. "Hydrated metal ions in aqueous solution: How regular are their structures? ." *Pure Applied Chemistry* 82 (2010): 1901-1917.
45. Rahbari, Ramine, Dominique Sarazin, and Jeanne Francois. "Interactions Between Acrylamide-Acrylic Acid Copolymers and Aluminum Ions in Aqueous Solutions ." *Oil Field Chemistry* , 1989: 124-136.
46. Ram, Arie, Ehud Finklestein, and Elata Chaim. "Reduction of Friction in Oil Pipelines by Polymer Additives." 1967: 309-313.
47. Ramsden, D.K, and K. McKay. "Degradation of Polyacrylamide in Aqueous Solution Induced by Chemically Generated Hydroxyl Radicals: Part I-Fenton's Reagent." *Polymer Degradation and Stability* , 1986: 217-229.
48. Schramm, Laurier. *Emulsions, Foams, Suspensions, and Aerosols: Microscience and Applications.* Weinheim : John Wiley & Sons , 2013.
49. Shah, S.N, and Ahmed Kamel. "Invesigation of Flow Behavior of Slickwater in Large Straight and Coiled Tubing ." *SPe Production & Operation*, 2010: 70-79.
50. Shah, Subhash, Ahmed Kamel, and Yunxu Zhou. "Drag Reduction Characteristics in Straight and Coiled Tubing-An Experimental Study ." *Journal of Petroleum Science and Engineering* , 2006: 179-188.
51. Shah, Subhash, and Aditya Vyas. "Temperature and Salinity Effects on Drag-Reduction Characteristics of Polymers in Coiled Tubing." *SPE* , 2011: 130685.

52. Shanshool, Jabir, and MT Haider. "Effect of Molecular Weight on Turbulent Drag Reduction with Polyisobutylene." *NUCEJ*, 2008: 52-59.
53. Shupe, Russel. "Chemical Stability of Polyacrylamide Polymers." *Journal of Petroleum Technology* , 1981: 1513-1529.
54. Sim, H.G. "Flow-induced chain scission in dilute polymer solutions: Algorithm development and results for scission dynamics in elongational flow." *Journal of Rheology*, 2007: 1223-1251.
55. Sreenivasan, Katepalli, and Christopher White. "The Onset of Drag Reduction by Dilute Polymer Additives, and the Maximum Drag Reduction Asymptote." *Journal of Fluid Mechanics*, 2000: 149-164.
56. Sworn, Graham. "Natural Thickeners ." In *Handbook of Industrial Water Soluble Polymers* , by Peter A. Williams, 10-31. Oxford: Blackwell Publishing , 2007.
57. Ting, Robert, and Oh-Kil Kim. "Drag-Reduction Properties of Ultra High-Molecular-Weight Polyacrylamide and Related Polymers ." In *Water-Soluble Polymers* , by N.M Bikales, 151-159. New Jersey : Plenum Press, 1973.
58. Toms, B.A. "Some observations on the flow of linear polymer solutions through straight tubes at large Reynolds numbers." *Proceedings of the 1st International Congressional Rheology*, 1948: 135-141.
59. Tucker, Kristen, and Paul McElfresh. "Could Emulsified Friction Reducers Prevent Robust Friction Reduction ." *SPE*, 2014: 168115.
60. USGS. "Produced Waters Database." *USGS.* 2012. http://www.usgs.gov/science/cite-view.php?cite=1259 (accessed 2014).
61. Verdu, Jaques. *Oxidative Aging of Polymers.* Wiley-ISTE, 2012.
62. Virk, P.S. "Drag Reduction Fundamentals ." *AIChE J.*, 1975: 625-656.
63. Walsh, M. "Theory of Drag Reduction in Dilute High-Polymer Flaws." *International Shipbuilding Progress*, 1967: 134.
64. Wikipedia. *Debye length.* June 26, 2014. http://en.wikipedia.org/wiki/Debye_length (accessed 12 19, 2014).
65. Williams, Peter. "Gelling Agents." In *Handbook of Industrial Water-Soluble Polymers*, by Peter Williams, 74-95. Oxford: Blackwelll Publishing , 2007.
66. —. *Handbook of Industrial Water Soluble Polymers* . Wiley-Blackwell, 2007.
67. Zhang, Rui, Zhongbin Ye, Li Peng, Ni Quin, Zheng Shu, and Pingya Luo. "The Shearing Effect on Hydrophobically Associative Water-Soluble Polymer and Partially Hydrolyzed Polyacrylamide Passing Through Wellbore Simulation Device ." *Applied Polymer Science*, 2010: 682-689.
68. Zhou, Jia, Hong Sun, and Qi Qu. "An Effecitve Model of Pipe Friction Prediction from Laboratory Characterization to Field Applicaitons for Friction Reducers." *Society of Petroleum Engineers*, 2011 : SPE 146674.
69. http://www.slideshare.net/diegonovoa/introduccin-bsicareologanovoa

Appendix

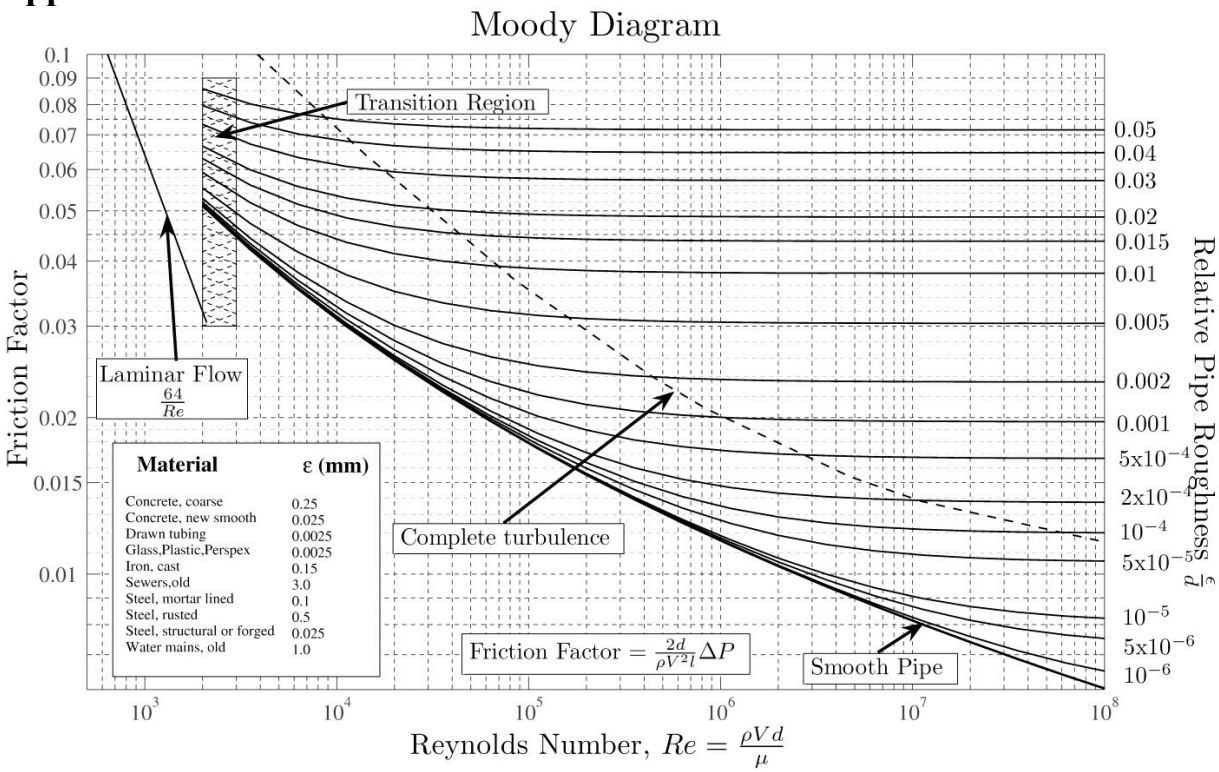

Appendix Figure 26- Moody Diagram [14]

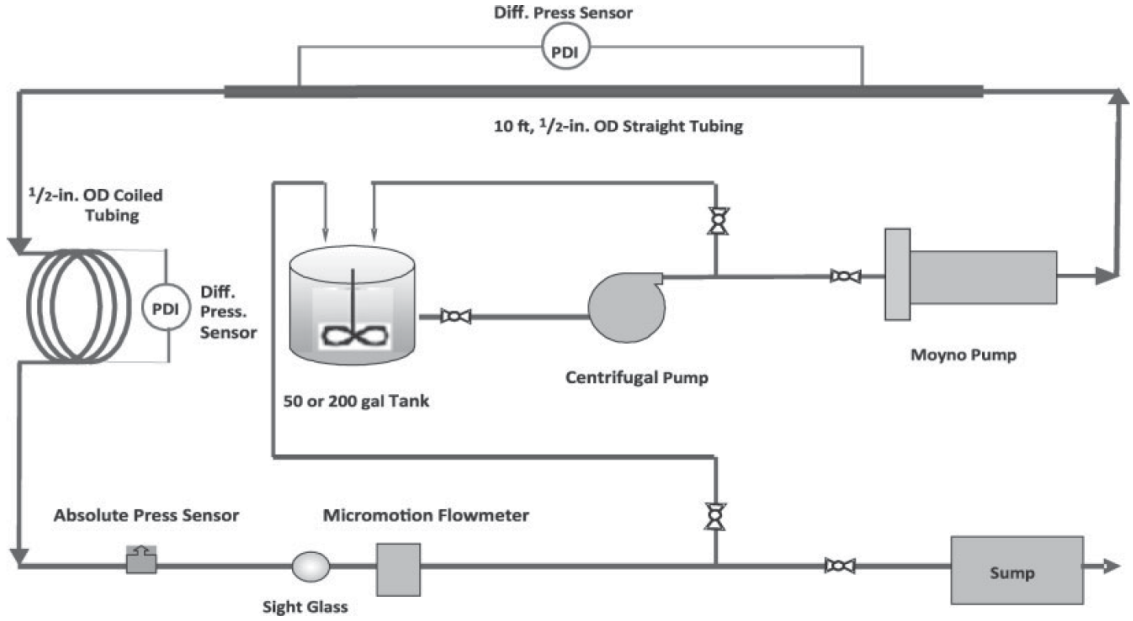

Appendix Figure 27-Friction Flow Loop Setup [51]L